REPORT DOCUMENTATION PAGE

Form Approved
OMB No. 0704-0188

Public reporting burden for this collection of information is estimated to average 1 hour per response, including the time for reviewing instructions, searching existing data sources, gathering and maintaining the data needed, and completing and reviewing this collection of information. Send comments regarding this burden estimate or any other aspect of this collection of information, including suggestions for reducing this burden to Department of Defense, Washington Headquarters Services, Directorate for Information Operations and Reports (0704-0188), 1215 Jefferson Davis Highway, Suite 1204, Arlington, VA 22202-4302. Respondents should be aware that notwithstanding any other provision of law, no person shall be subject to any penalty for failing to comply with a collection of information if it does not display a currently valid OMB control number. **PLEASE DO NOT RETURN YOUR FORM TO THE ABOVE ADDRESS.**

1. REPORT DATE *(DD-MM-YYYY)*	**2. REPORT TYPE**	**3. DATES COVERED** *(From - To)*
13-12-2006	Journal Article	

4. TITLE AND SUBTITLE

Mechanical Properties for an Arbitrary Arrangement of Rigid Spherical Particles Embedded in an Elastic Matrix (Preprint)

5a. CONTRACT NUMBER
F04611-98-C-0005

5b. GRANT NUMBER

5c. PROGRAM ELEMENT NUMBER

6. AUTHOR(S)
Robert L. Hatch & I. Lee Davis (ATK Launch Systems Group)

5d. PROJECT NUMBER
101100NF

5e. TASK NUMBER

5f. WORK UNIT NUMBER

7. PERFORMING ORGANIZATION NAME(S) AND ADDRESS(ES)

ATK Launch Systems
P.O. Box 707
Brigham City UT 84302-0707

8. PERFORMING ORGANIZATION REPORT NUMBER

AFRL-PR-ED-JA-2007-076

9. SPONSORING / MONITORING AGENCY NAME(S) AND ADDRESS(ES)

Air Force Research Laboratory (AFMC)
AFRL/PRS
5 Pollux Drive
Edwards AFB CA 93524-70448

10. SPONSOR/MONITOR'S ACRONYM(S)

11. SPONSOR/MONITOR'S NUMBER(S)
AFRL-PR-ED-JA-2007-076

12. DISTRIBUTION / AVAILABILITY STATEMENT

Distribution A: Approved for public release; distribution unlimited (PA # 07239A).

13. SUPPLEMENTARY NOTES
Submitted for publication in the Journal of the Physics and Mechanics of Solids.

14. ABSTRACT

A computer code has been written which calculates the small deformation stress and strain fields of a medium consisting of a pack of rigid spherical particles embedded in an elastic Hookean matrix. The stress and strain tensors can be calculated at any point in the medium to within a user-specified accuracy. Average mechanical properties of the medium are also output by the code. The code has been used to simulate systems consisting of thousands of particles in a finite pack. Optionally, the code treats an infinite pack made up of repeating 3D rectangular cells of a particle pack. The multipole expansion technique used to solve the equations of small deformation for the elastic medium consists of truncated sums of complete orthogonal vector spherical harmonics. Techniques are presented which improve the convergence of the solution when the particles are in close proximity for highly filled materials. The code has been tested against exact solutions of configurations consisting of a few particles as well as infinite packs of particles in body-centered cubic, face-centered cubic, and simple cubic lattice arrangements. The code has been used to estimate mechanical properties of a variety of monomodal and bimodal particle packs of different packing densities for a matrix material with a variety of elastic constants.

15. SUBJECT TERMS

16. SECURITY CLASSIFICATION OF:			**17. LIMITATION OF ABSTRACT**	**18. NUMBER OF PAGES**	**19a. NAME OF RESPONSIBLE PERSON**
					Dr. Gregory Ruderman
a. REPORT	**b. ABSTRACT**	**c. THIS PAGE**	SAR	69	**19b. TELEPHONE NUMBER** *(include area code)*
Unclassified	**Unclassified**	**Unclassified**			

Mechanical properties for an arbitrary arrangement of rigid spherical particles embedded in an elastic matrix (Preprint)

Robert L. Hatch and I. Lee Davis

ATK Launch Systems, Brigham City, UT 84302-0707, U.S.A.

Abstract

A computer code has been written which calculates the small deformation stress and strain fields of a medium consisting of a pack of rigid spherical particles embedded in an elastic Hookean matrix. The stress and strain tensors can be calculated at any point in the medium to within a user-specified accuracy. Average mechanical properties of the medium are also output by the code. The code has been used to simulate systems consisting of thousands of particles in a finite pack. Optionally, the code treats an infinite pack made up of repeating 3D rectangular cells of a particle pack. The multipole expansion technique used to solve the equations of small deformation for the elastic medium consists of truncated sums of complete orthogonal vector spherical harmonics. Techniques are presented which improve the convergence of the solution when the particles are in close proximity for highly filled materials. The code has been tested against exact solutions of configurations consisting of a few particles as well as infinite packs of particles in body-centered cubic, face-centered cubic, and simple cubic lattice arrangements. The code has been used to estimate mechanical properties of a variety of monomodal and bimodal particle packs of different packing densities for a matrix material with a variety of elastic constants.

Distribution A: Approved for public release; distribution unlimited.

1. Introduction

Mechanical models of particulate materials can be categorized in several ways.

- Particle properties: isotropic, rigid particles, deformable particles, voids
- Particle shape (Davis, 1999): spherical (Goodier, 1933; Walpole, 1972), ellipsoidal (Robinson, 1951; Edwards, 1951; Eshelby, 1957; Buchalter, 1994), irregular (Yamamoto, et al., 1999), chopped fiber (Lopez-Pamies, 1996)
- Matrix properties: isotropic, linearly elastic, nonlinear elastic (Chen, et al., 1993), nonlinear viscoelastic (Schapery, 1986) ;Matous, et al., 2005), nonlinear viscoplastic (Olsen et al., 1998)
- Particle-matrix bond: bond strength less than (Gent, 1980) or greater than (Gent et al., 1984) matrix failure strength (T. Smith, 1959; Sangani, 1997)
- Microstructure evolution: microstructure changes (e.g., particle debonding) or does not change with application of boundary condition history such as loads, temperatures, and chemical environments
- Computational efficiency: empirical models (van der Poel, 1958; Hashin, 1964; J. Smith, 1974, 1975, 1976), semi-empirical and bounded models (Hashin, 1983; Christensen, 1990; Aravas, 2005), special case models (Sangani, 1987), physics-based models with simplified microstructural input (Christensen, 1990; Vratsanos, 1993), intensive physics-based models with detailed microstructural input (Davis, et al., 1993; Phan-Thien et al., 1994; Torquato, 1997)

Many users of particulate material models need mechanical constitutive models that can be placed into a finite element code to predict the integrity of structures partially or wholly comprised of particulate composites. The constitutive relation should satisfy

three criteria: (1) reasonable accuracy, (2) computational tractability, and (3) numerical stability. Unfortunately, computational tractability and reasonable accuracy are difficult to simultaneously obtain. The more microstructural information one puts into a model, the more accurate it can be, but the more computationally intensive it will become.

The construction of a routinely usable particulate model therefore becomes a search for those physical phenomena that have greatest impact for the least computational burden. In order to filter through the most influential physical phenomena, we must have models that may themselves be too detailed and computationally intensive for practical use, but can guide and validate simpler models. With a detailed model, one can quantify the accuracy and computational or stability gain for each simplifying assumption. Broad treatments with many references on particulate theories and modeling issues may be found in Christensen (1979), Cusak (1987), and Torquato (2002).

In this paper, we describe a computationally intensive model for rigid, bonded, spherical particles in an isotropic, linearly elastic matrix using Navier multipoles. Later papers will present our efforts at computationally tractable statistical mechanical models condensed from the detailed treatment of this paper and with added microstructural detail such as debonding particles, viscoelastic and large deformation matrix materials, and nonspherical particles.

When the authors first employed a multipole expansion technique to treat the mechanical response of a particulate material (Davis, et al., 1993), several dozen particles could be efficiently modeled with Navier multipoles. Since that early effort, another project was launched to refine and enhance the capabilities of the method. A more elegant mathematical foundation based on vector spherical harmonics was adopted that

greatly simplified the multipole expansion method. This formalism led to the straightforward implementation of addition theorems that give the solutions in terms of a large number of linear algebraic equations. The use of addition theorems allows several efficiency measures to be incorporated into the solution of the problem so that thousands of particles in a highly filled medium can be efficiently modeled on current computers. An efficient technique was devised to treat the interaction between particles of very close proximity with very high order multipole terms.

The original paper treated a finite collection of particles. The method has since been extended to approximate an infinite medium with repeating 3D rectangular cells of particles. The mathematical methods described in this paper are programmed in the PARMECH computer code.

Independently, work was carried along similar lines by other researchers. Kushch (1997) used a multipole expansion technique to model aligned spheroidal particles (not necessarily rigid) in periodic repeating unit cells. Addition theorems were used to reduce the problem to an algebraic system of equations. Numerical solutions were given for a single particle in a unit cell corresponding to a periodic lattice.

Sangani and Mo (1997) also used a multipole expansion technique to treat repeating cells of spherical particles. Accurate calculations were made of highly-filled systems containing up to 32 random particles of a single size in the unit cell.

Despite the previous work in this area, there is a lack of calculations of model systems that can be used to guide the construction of particulate constitutive models. In particular, the authors found no systematic calculations treating systems where the particles differed in size by a significant amount. Of course such systems are challenging

because of the large number of small particles that must be included when a statistically significant number of larger particles are treated. Nevertheless, such calculations are critical in validating models that treat collections of particles of different sizes.

Most of the calculations presented in this paper are for a matrix material with Poisson's ratio near ½. When the particles are in close proximity, the stress concentrations between close particles are particularly large for this condition. To treat these concentrations accurately with a multipole expansion technique is a challenge and highlights the efficiency of the nearest neighbor treatment that allows the effective treatments of particles in close proximity.

In this paper the mathematical formulation based on vector spherical harmonics of the multipole expansion technique is summarized. It is shown how the addition theorems can be applied to the governing equations to satisfy the appropriate boundary conditions. Efficiency measures implemented into the code are explained and the nearest neighbor treatment is derived. Next, a comparison of predictions of the PARMECH code is made with exact solutions for a simple two-particle system as well as infinite repeating lattice arrangements of particles. Predictions of the code for random arrangements of particles are also presented. We treat in detail systems containing a single particle size and also two distinct particle sizes.

2. Elements of particulate models

Three questions that should be addressed when building a microstructural particulate model are

(1) What are the relevant properties of the individual phases?

(2) How are the phases geometrically arranged relative to each other?

(3) What are the laws of interaction among the phases when subject to boundary conditions of interest?

Within the scope of our work, we will answer the first question in this section, the second question in Section 3, and the third question in Section 4.

In the particulate composites of interest to us, the particle Young's modulus is orders of magnitude higher than matrix modulus. Hence we treat the particles as rigid. However, we emphasize that our multipole formalism works equally well for a set of nonrigid particles, each with its own Lamé constants. The algebra involved roughly doubles but the conceptual framework is no more complicated.

We treat the matrix as an isotropic, Hookean solid described by the two elastic Lamé constants, λ and μ. These two constants are input to the model.

We will treat the case where the particles are initially bonded and stay bonded to the matrix. Again, the Navier multipole formalism can treat particles that debond from the matrix after a certain threshold criterion is met. However, since there are a variety of boundary conditions that can be applied to debonding particles, there is much experimental and theoretical work still needed to write the simulation code for debonding particulate materials. We have worked through some of the algebra on several debonding scenarios but these treatments are not programmed or mature enough to present here. We hope to present them in subsequent work. It is clear, however, that the computational burden will increase substantially, more than an order of magnitude, when debonding is permitted. It is also clear that the nature of debonding and the subsequent particle-matrix boundary conditions for a given particulate material is not trivial to characterize.

3. Random particle packing with arbitrarily broad particle size distributions

To make detailed microstructural calculations of particulate materials, one must have the detailed microgeometry of the particle pack. Hence a particle-packing algorithm must be available which can place a sufficiently large number of particles to create a faithful statistical sampling of a full pack. Many packing algorithms exist (Davis, 1999). Two important categories of particle packing models are ballistic deposition and molecular dynamics. In ballistic deposition, the particles are added to the pack one at a time. Each particle rolls about on the pack until it finds a stable equilibrium point resting upon other particles of the pack and/or upon a simulated container wall. In molecular dynamics (as the name implies), the particles are placed in a container and allowed to move and collide with each other and the container wall as the wall slowly closes them into a close pack configuration. The ballistic deposition algorithms are computationally much faster but do not pack to as high a packing density as the molecular dynamics methods. A third category of packing algorithms grows the particles from randomly distributed seeds (Kochevets et al., 2001) which then move to avoid overlap as growth causes them to bump into each other.

The importance of the packing algorithm can hardly be overemphasized when dealing with particulate composites that are near close pack. In close pack, the particles are nearly touching, that is, the mean surface-to-surface distance is much less that the particle radii. The mechanical properties near close pack are ruled by the large stress concentration spikes that occur between nearly touching, rigid particles (Figure 1). The

height and size of the stress concentration spikes are ruled by the distribution of surface-to-surface distances, being inversely proportional to the surface-to-surface distance for

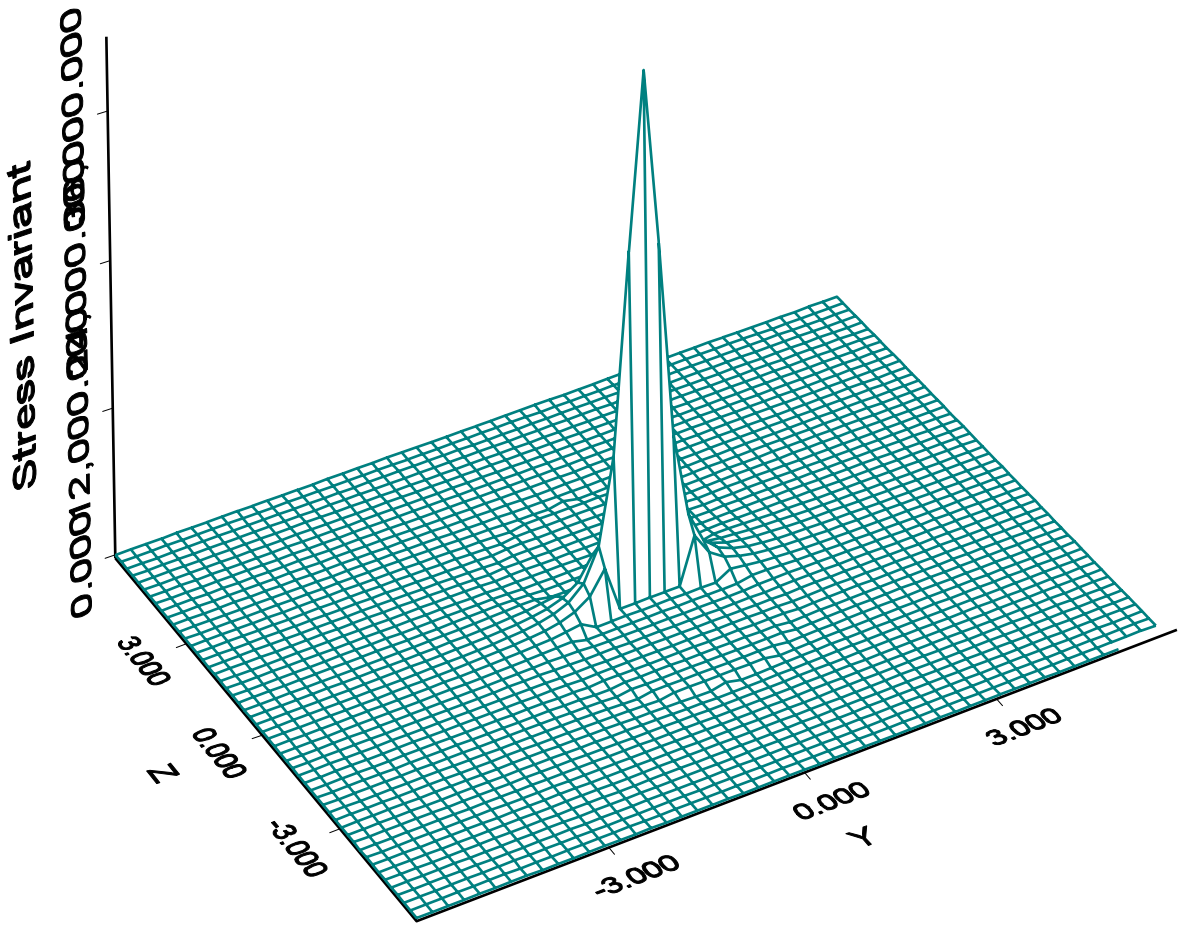

Figure 1. Stress concentration spike (trace of the stress tensor) plotted for the region around two rigid spheres embedded in a nearly incompressible matrix under uniaxial tension in the *z* direction. These spikes dictate mechanical properties in highly filled particulate materials.

nearly incompressible matrix material. From experience, we have learned that even though a packing algorithm may give the correct volume fraction of particles, if it does not mimic the actual surface-to-surface distance distribution of the real material, the predicted mechanical properties can be in error by a few hundred percent. A

considerable burden is therefore placed on the researcher to understand how the real pack was constructed and adapt packing algorithms that yield the same surface-to-surface distance distributions with good fidelity.

The particle packs of interest to us have broad size distributions. Most packing algorithms cannot treat broad distributions because of the simple problem of numbers. Consider a bimodal pack where the two particle sizes differ by a factor of one hundred. Suppose the coarse and fine modes are roughly equivalent in volume quantity. Then, since the particle diameters differ by 10^2, the particle volumes differ by 10^6. If one must place several thousand coarse particles to get a reasonable statistical sampling of the pack, it follows one must place $10^6\times$(several thousand) = several billion small particles to fill the interstitial spaces of the larger particles.

To circumvent this problem, we devised a scheme called a reduced-dimension packing algorithm (Davis et al., 1990), the short-comings of which have been recently corrected (Webb et al., 2006) to provide a robust packing code PARPACK for broader size distributions than are currently available in other packing codes (Figure 2). On current desktop computers, PARPACK can create simple packs with a few million particles (far more than is generally needed to obtain the statistical flavor of simple packs) in a few minutes and more complex packs of the same size in a few hours. PARPACK can also generate coordination numbers for the modes of the pack and their radial distribution functions. Generating higher-order statistical functions would be a simple matter but has not been done at this point.

We use PARPACK to generate packs used by the PARMECH code described in this paper.

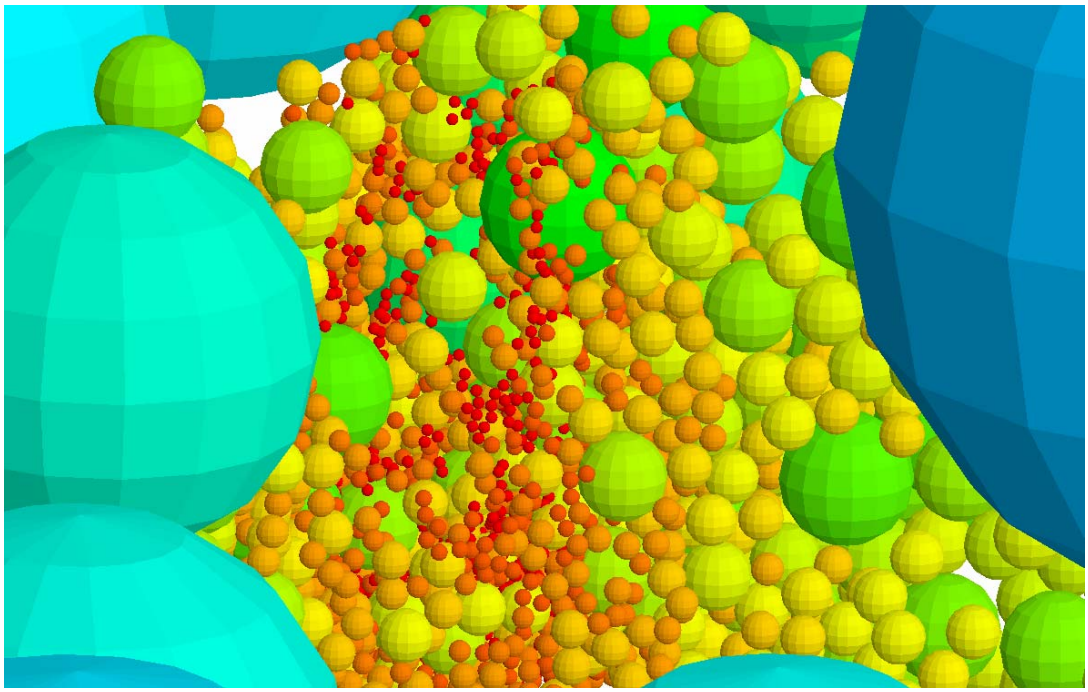

Figure 2. Visualization of a reduced dimension pack. The smaller particles are constrained to lie close to the pack axis. Then the statistics of the inner small particle columns are projected into the outer part of the pack where the larger particles place themselves according to small particle statistics. Hence, large particles lying in the outer regions of the pack respond to small particle statistics rather than billions of small particles themselves. In this way we mimic full 3D pack statistics with broad size distribution with a tiny fraction of the particles needed in a 3D pack. This cut-away picture peers past some large particles into the small-particle core of the pack.

4. The laws of interaction

In this section we describe the mathematical foundations of the multipole method of solution used by the PARMECH code. In subsequent sections, we discuss efficiency measures employed by the code to speed the solution process. We also summarize the capabilities of the code.

4.1 General solution of the Navier equation

The Navier equation for elastic, isotropic, Hookean material is given by

$$(\lambda + 2\mu)\nabla(\nabla \cdot \vec{u}) - \mu \nabla \times \nabla \times \vec{u} = 0 \tag{1}$$

where λ and μ are the Lamé constants. The small deformation displacement vector is denoted by $\vec{u}$. Cartesian components will be used for all displacement vectors so that they may be readily added when the interactions of many spheres are included. However, each Cartesian component of $\vec{u}$ is in spherical polar coordinates (r,θ,φ) centered on the *i*-th sphere, which that particular displacement vector field is describing:

$$u_k^i = u_k^i(r,\theta,\varphi) \quad , k = x, y, z \, . \tag{2}$$

A general solution to the Navier equation for the region outside a sphere *i* of radius *a* is

$$\vec{u}^{\,i}(\vec{r}) = \sum_{L=0}^{\infty} \sum_{n=L-1}^{L+1} \sum_{m=-n}^{n} B_{L,nm}^i \vec{u}_{L,nm}(\vec{r}) \tag{3a}$$

$$\vec{u}_{L,nm}(\vec{r}) = \vec{V}_{L,nm}(\vec{r}) + d_n(r^2 - a^2)\nabla[\nabla \cdot \vec{V}_{L,nm}(\vec{r})] \tag{3b}$$

$$\vec{V}_{L,nm}(\vec{r}) = \left(\frac{a}{r}\right)^{L+1} \vec{Y}_{nm}^L(\theta,\varphi) \tag{3c}$$

$$d_n = \frac{\lambda + \mu}{2[\lambda + 2\mu + (\lambda + 3\mu)n]} \tag{3d}$$

$$(r^2 - a^2)\nabla[\nabla \cdot \vec{V}_{L,nm}(\vec{r})] = \tag{3e}$$

$$\begin{cases} -(2n-1)\sqrt{n(n+1)}\left[\left(\frac{a}{r}\right)^n - \left(\frac{a}{r}\right)^{n+2}\right]\vec{Y}_{nm}^{n+1} & , L = n-1 \\ 0 & , L = n \text{ or } n+1 \end{cases}$$

where the constants $B_{L,nm}^i$ are called the multipole moments for sphere *i* and *r* is the distance from the center of the sphere ($r \geq a$). The $\vec{Y}_{nm}^{L}(\theta,\varphi)$ are vector spherical harmonics defined by (Varshalovich et al., 1988, p. 210)

$$\vec{Y}_{nm}^{L}(\theta,\varphi) = \sum_{m',k} C_{Lm'1k}^{nm} Y_{Lm'}(\theta,\varphi)\hat{\mathbf{e}}_k \tag{4}$$

where the unit vectors are defined by

$$\begin{aligned} \mathbf{e_{-1}} &= (\mathbf{e_x} - i\mathbf{e_y})/2^{1/2} \\ \mathbf{e_0} &= \mathbf{e_z} \\ \mathbf{e_{+1}} &= -(\mathbf{e_x} + i\mathbf{e_y})/2^{1/2} \quad , \end{aligned} \tag{5}$$

the $C_{Lm'1k}^{nm}$ are Clebsch-Gordon coefficients, and the Y_{Lm} are scalar spherical harmonics. These vector spherical harmonics are orthonormal

$$\int_0^{2\pi} d\varphi \int_{-1}^{1} d(\cos\theta)\, \vec{Y}_{n'm'}^{L'*} \cdot \vec{Y}_{nm}^{L} = \delta_{LL'}\delta_{nn'}\delta_{mm'} \quad , \tag{6}$$

and complete, in that there always exists a unique set of coefficients $A_{L,nm}$ in which any arbitrary piecewise continuous vector function $\vec{F}(\theta,\varphi)$ can be expanded:

$$\vec{F}(\theta,\varphi) = \sum_{L=0}^{\infty} \sum_{n=L-1}^{L+1} \sum_{m=-n}^{n} A_{L,nm} \vec{Y}_{nm}^{L}(\theta,\varphi) \quad . \tag{7}$$

The Navier solution (3) about a sphere simplifies considerably at $r = a$:

$$\vec{u}^i(\vec{r})\Big|_{|\vec{r}|=a} = \sum_{L=0}^{\infty}\sum_{n=L-1}^{L+1}\sum_{m=-n}^{n} B^i_{L,nm}\vec{Y}^L_{nm}(\theta,\varphi)\,. \tag{8}$$

The completeness of the vector spherical harmonics implies that any displacement field obeying the Navier equation about a sphere can be described, from a simple translational displacement of a bonded sphere to a complex displacement for an unbonded sphere. Only the bonded sphere is treated in this paper. The orthonormality of the vector spherical harmonics allows the boundary condition about a sphere to be applied without the need for time-consuming numerical integrations.

The general solution to the Navier equation for *N* spherical particles can be written as

$$\vec{u}(\vec{r}) = \sum_{i=1}^{N}\vec{u}^{\,i}(\vec{r}-\vec{r}_i) + \sum_{n=0}^{2}\sum_{m=-n}^{n} F_{nm} r\vec{Y}^1_{nm}(\theta,\varphi)\,, \tag{9}$$

where $\vec{r}_i$ is the position of particle *i*. The first sum in (9) is a sum of single particle solutions defined in (3) and goes to zero as r $\rightarrow \infty$. The second sum represents the applied field far from the particles with F_{nm} derived from the applied strains. The specific solution to a given problem is therefore obtained by determining the coefficients $B^i_{L,nm}$ of (3) that satisfy the boundary conditions for the problem.

4.2 Boundary conditions and addition theorems

The PARMECH code currently treats the problem for which the particles are bonded to the matrix material. The boundary condition at the surface of a particle is given by a rigid displacement and rotation of the particle surface and can be written as

$$\vec{u}^i(\vec{r})\Big|_{|\vec{r}|=a} = \sum_{m=-1}^{1}\left(\gamma^i_m\vec{Y}^0_{1m}(\theta,\varphi) + \psi^i_m\vec{Y}^1_{1m}(\theta,\varphi)\right), \tag{10}$$

where the first term in the sum gives the translation of the surface and the second term gives the rotation of the surface.

Large computation efficiency is achieved through the powerful mathematical relationship of addition theorems that expresses a vector spherical harmonic about a point $\vec{r}_j$ in terms of a sum of vector spherical harmonics about a point $\vec{r}_i$. This allows the general solution (9) evaluated at the surface of sphere *i* to be rewritten in terms of a sum of vector spherical harmonics with coordinates centered about the point $\vec{r}_i$ as

$$\vec{u}^i(\vec{r})\Big|_{\|\vec{r}\|=a} = \sum_{L,n,m}\left[B^i_{L,nm} + \sum_{\substack{j=1\\ j\neq i}}^{N}\sum_{L',n'm'} B^j_{L',n'm'} C^{L',n'm',ij}_{L,nm}\right]\vec{Y}^L_{nm}(\theta,\varphi) + \sum_{L=0}^{1}\sum_{n=L-1}^{L+1}\sum_{m=-n}^{n}\sum_{n'=0}^{2}\sum_{m'=-n'}^{n'} F_{n'm'} f^{n'm',ij}_{L,nm}\vec{Y}^L_{nm}(\theta,\varphi) \tag{11}$$

where

$$\sum_{L,n,m} \equiv \sum_{L=0}^{\infty}\sum_{n=L-1}^{L+1}\sum_{m=-n}^{n} \tag{12}$$

and the off-center expansion coefficients $C^{L',n'm',ij}_{L,nm}$ and $f^{n'm',ij}_{L,nm}$ are derived from the addition theorems of the spherical harmonics and depend only on the geometry of the particle pack. Their derivation is given in Appendix A.

The boundary conditions are now easily applied by setting (10) equal to (11) and applying the orthonormality condition of (6), then rearranging terms to obtain the following set of linear equations:

$$B^i_{L,nm} = \gamma^i_m \delta_{L0}\delta_{n1} + \psi^i_m \delta_{L1}\delta_{n1} - \sum_{\substack{j=1\\ j\neq i}}^{N}\sum_{L',n'm'} B^j_{L',n'm'} C^{L',n'm',ij}_{L,nm} - \sum_{n'=0}^{2}\sum_{m'=-n'}^{n'} F_{n'm'} f^{n'm',ij}_{L,nm} \; . \tag{13}$$

Given the displacements γ_m^i and rotations ψ_m^i, (13) can be solved for the coefficients $B_{L,nm}^i$, thus completely specifying the displacement vector field and providing a complete solution to the problem.

The solution process is easily modified if the rotations and displacements are not specified but that the particles are in equilibrium (i.e., forces and torques on each particle are zero) is specified. For this case it can be shown that

$$B_{0,1m}^i = 0 \quad \textit{and} \quad B_{1,1m}^i = 0, \quad \text{(force and torque on particle } i \text{ are zero).} \tag{14}$$

The displacements γ_m^i and rotations ψ_m^i can then be determined from (13).

4.3 Efficiency measures and nearest-neighbors treatment

When solving (13), the sums can be truncated at some maximum value L_{max} depending on the desired accuracy of the solutions. It is important to truncate this sum at the lowest reasonable value since the number of terms N_{mp} in a given particle's multipole expansion grows as

$$N_{mp} = 3(L_{max}+1)^2 . \tag{15}$$

When stress concentrations in the problem are large, as they are for packs where the particles are in close proximity, a large value of L_{max} is required for good accuracy. The values of L_{max} that are required for a given accuracy are discussed in later sections.

Another efficiency measure is possible by looking at the form for the off-center expansion coefficients

$$C_{L,nm}^{L',n'm',ij} \propto \frac{a_i^L a_j^{L'+1}}{R_{ij}^{L+l'+1}}, \tag{16}$$

where R_{ij} is the distance between spheres i and j. Thus, the off-center expansion coefficients become small when the particles are far apart for large values of L and L' which allows an earlier truncation of the sum.

A further important efficiency measure, which we refer to as the nearest-neighbors treatment, is included in the code to allow an accurate treatment of particles when they are in close proximity. This approximation is of value when the Poisson's ratio is near 0.5.

The greatest stress concentration in a particle pack is in the region between two nearly touching particles. The stress concentrations are particularly high when the Poisson's ratio of the matrix material is near 0.5 and there is an axial displacement of the two particles. The asymptotic load transfer between the two spheres in that case is proportional to ε^{-1}, where ε is a dimensionless distance between the sphere surfaces. On the other hand, when the Poisson's ratio is not near 0.5 or for a shear displacement between particles when Poisson's ratio is near 0.5, the asymptotic load transfer (Phan-Thien et al., 1994, Ch. 4) is proportional to $\ln(\varepsilon^{-1})$.

These two-body interactions can be described with a large number of multipoles separately from the remainder of the pack. For some calculations, while the general pack used an L_{max} of 12, the nearest-neighbors treatment used an L_{max} of 200 for the two-body interaction only.

We let NN_i be the set of nearest neighbors of particle i and write the multipole expansion coefficients of particle i as

$$B^i_{L,nm} = \gamma^i_m \delta_{L0}\delta_{n1} + \psi^i_m \delta_{L1}\delta_{n1} + \sum_{j\in NN_i} \widehat{B}^{i,j}_{L,nm} + A^i_{L,nm} \ . \tag{17}$$

The first two terms on the right hand side of (17) describe the displacement and rotation of particle *i*, the $\widehat{B}^{i,j}_{L,nm}$ represents the contribution due to the tensile interaction of particle *i* with particle *j* and must be treated with high order, and the $A^i_{L,nm}$ give the remaining contribution to the multipole coefficients and need not be treated with high order.

If we substitute (17) into (13) for the nearest neighbors of particle *i* we obtain the following relationship:

$$\begin{aligned}
&\sum_{j\in NN_i}\widehat{B}^{i,j}_{L,nm}+A^i_{L,nm}\\
&\quad=-\sum_{j\in NN_i}^{N}\sum_{L',n'm'}\left(\gamma^j_{m'}\delta_{L'0}\delta_{n'1}+\psi^j_{m'}\delta_{L'1}\delta_{n'1}+\sum_{k\in NN_j}\widehat{B}^{j,k}_{L',n'm'}+A^j_{L',n'm'}\right)C^{L',n'm',ij}_{L,nm}\\
&\qquad-\sum_{j\notin NN_i}^{N}\sum_{L',n'm'}B^j_{L',n'm'}C^{L',n'm',ij}_{L,nm}-\sum_{n'=0}^{2}\sum_{m'=-n'}^{n'}F_{n'm'}f^{n'm',i}_{L,nm}\quad .
\end{aligned}\tag{18}$$

Now $\widehat{B}^{i,j}_{L,nm}$ is defined as the solution to (8) when there are only two neighboring particles (other particles are not present) and their displacement is purely tensile with no rotation or far field. Thus,

$$\widehat{B}^{i,j}_{L,nm}=-\sum_{L',n'm'}\left(\widehat{B}^{j,i}_{L',n'm'}+\gamma^{t,j,i}_{m'}\delta_{L'0}\delta_{n'1}\right)C^{L',n'm',ij}_{L,nm}\ ,\tag{19}$$

where the tensile component of displacement is given by

$$\vec{\gamma}^{\,t,j,i}=\left(\frac{\vec{r}_{ji}\cdot\left(\vec{\gamma}^{\,j}-\vec{\gamma}^{\,i}\right)}{2\vec{r}_{ji}\cdot\vec{r}_{ji}}\right)\vec{r}_{ji}\tag{20}$$

with $\vec{r}_{ji}=\vec{r}_j-\vec{r}_i$ the vector pointing from the center of particle *i* to the center of particle *j*.

We can substitute (19) into the left hand side of (18) and solve for $A^i_{L,nm}$ as

$$A^i_{L,nm} =$$

$$-\sum_{j\in NN_i}^{N}\sum_{L',n'm'}\left(\left(\gamma^j_{m'}-\gamma^{t,j,i}_{m'}\right)\delta_{L'0}\delta_{n'1}+\psi^j_{m'}\delta_{L'1}\delta_{n'1}+A^j_{L',n'm'}+\sum_{\substack{k\in NN_j\\k\neq i}}\widehat{B}^{j,k}_{L',n'm'}\right)C^{L',n'm',ij}_{L,nm} \qquad (21)$$

$$-\sum_{j\notin NN_i}^{N}\sum_{L',n'm'}B^j_{L',n'm'}C^{L',n'm',ij}_{L,nm}-\sum_{n'=0}^{2}\sum_{m'=-n'}^{n'}F_{n'm'}f^{n'm',i}_{L,nm}$$

Subtracting out the tensile component from the displacement in (21) allows the use of much lower values of L because only shear displacements remain for the nearest neighbors. In the computer code, we solve (19) to high order in L. This is facilitated by solving (19) for a unit displacement in a reference frame where the two particles are aligned along the z axis so that there is cylindrical symmetry and only $m = 0$ values are required in the multipole expansion, thus reducing the number of multipole terms from $O(L_{max}^2)$ to $O(L_{max})$. The $\widehat{B}^{i,j}_{L,nm}$ are then derived from the calculated $\widehat{B}^{i,j}_{L,n0}$ by applying the proper rotation using well-known rotation properties of the vector spherical harmonics (Varshalovich et al., 1988) and scaling according to the actual displacement of the particles. The coefficients $A^i_{L,nm}$ are calculated from (21) through an iterative procedure and used in (17) to calculate the multipole coefficients $B^i_{L,nm}$.

The nearest neighbor treatment allows the use of a much smaller L_{max} for an accurate treatment of a particle pack and hence greatly reduces the memory requirements and computational time for each iteration. However, the number of iterations required to reach convergence is increased. In a later section we compare the treatment of particle packs with and without the nearest neighbor treatment and demonstrate the computational advantages of using this efficiency measure for highly filled packs.

5. Infinite particle packs consisting of repeating cells of particles

Up to this point we have discussed the theory for a system consisting of a finite number of particles *N*. The PARMECH code also treats pseudo-infinite systems where the particle configuration is made by stacking a cell into a three-dimensional grid of rectangular unit cells consisting of *N* particles. The centers of all the particles must fit inside the unit cell in such a way that particles do not overlap with particles of the neighboring cell. A slice through two neighboring unit cells of particles is shown in Appendix B.

The formalism remains as described above with the contribution from other cells included in the off-center expansion coefficients. Thus, the "pseudo-infinite" system is actually a very large finite system made up of the repeated unit cells that consists of an inner region where the relative displacement fields in each of the cells is identical. This inner region is much larger than the dimension of the unit cell.

Only the multipole coefficients $B^i_{L,nm}$ for the unit cell need be treated, but the off-center expansion coefficients $C^{L',n'm',ij}_{L,nm}$ must include contributions from each of the neighboring cells. Appendix B describes an efficient technique to calculate the off-center expansion coefficients.

6. Mechanical properties of a collection of particles

The code will estimate the mechanical properties of a random finite collection of particles in an approximately spherical geometry. Given a random spherical finite pack of particles and uniaxial strains in the elastic medium far from the particles, the code calculates the displacement of each particle in the pack as well as estimates an effective

modulus and Poisson's ratio for the pack. This assumes the pack is isotropic. The mechanical properties of the pack are determined by a fit to the exact solution of a spherical body embedded in an elastic medium (Goodier, 1933). Details are given in Appendix C.

For an infinite pack, the mechanical properties of the system are determined from the average stress and strain tensor seen in the unit cell, and are derived in Appendix D.

7. Method of solution of the linear set of equations

We employ an iterative method of solution for the linear set of equations (13). An initial guess is provided for all $B^i_{L,nm}$, that guess being those multipole moments appropriate for an isolated sphere in an infinite medium with uniform applied fields. The $B^i_{L,nm}$ for each particle *i* is then recalculated by setting its value equal to the right hand side of (13). The convergence can be surprisingly fast depending on how close the particles are. For example, a 13000-particle pack with a volume concentration of particles $C = 0.10$ will converge in 16 iterations while a large pack with volume concentration of $C = 0.50$ may take more than 100 iterations to converge.

8. Results

In this section we summarize some of the simulations that have been done with the PARMECH code. We begin by comparing the code results to exact calculations of model systems that have been studied in the literature. This includes forces on two spherical particles and systems made up of spherical particles arranged as infinite cubic lattices.

We also present results for random arrangements of monomodal and bimodal packs of particles. Care was taken in the construction of dense packs to prevent building into the packs order that would result in artificial crystallinity. The packs were generated with a method to build a pack of touching particles (Webb et al., 2006). The pack was then allowed to expand into a fixed volume, keeping all particle sizes constant, using a random ballistics/collision dynamic simulation. The dynamic randomization was run long enough to allow the total distance of travel of a particle to be many times the distance across the confining volume. The result is a detailed knowledge of the material microgeometry, with a user-specified volume fraction (always less than the packing fraction), consistent with fully random fabrication of the material.

8.1 Simple two-particle system

To study the convergence of the multipole solutions and the accuracy obtained for a given L_{max}, we compared our solutions with exact two-sphere solutions derived in bispherical coordinates by Shelley and Yu (1966). Table I shows the excellent agreement of the PARMECH predictions with the exact bispherical solutions. The parameter ε, mentioned earlier, is a dimensionless variable that indicates the proximity of the spheres and is defined as

$$\varepsilon = \text{(surface-to-surface distance)/(diameter of smallest sphere)}. \tag{22}$$

As expected, when the spheres are close together, much higher L_{max} is required to achieve high accuracy, hence the importance of the nearest neighbors treatment discussed in previous sections.

Table I. Comparison of PARMECH Predictions with Exact Results for the Forces between Two Equal Sized Spheres With Equal and Opposite Uniaxial Displacements

Matrix Poisson Ratio σ = 0.5

Particle Proximity ε	Exact Force	PARMECH Calculated Force	Error (%)	L_{max}
1.0	3009.6747	3009.6747	0.0	4
0.1	8718.9434	8686.6202	0.4	8
		8718.8904	0.0006	16
		8718.9417	0.00002	26
0.01	52993.6830	47477.	10.	21
		50694.3	4.	26
		52982.554	0.02	50
		52993.6830	0.0	100
0.001	479048.65	474229.41	1.0	200
		479048.55	0.00002	400

8.2 Infinite cubic lattice arrangements of particles

In order to provide a rigorous testing of the code, we have compared the code results to calculations in the literature for infinite lattice arrangements of SC, BCC, and FCC symmetry (Nunan et al., 1984; Sangani et al., 1987). For these cubic lattices the effective elasticity tensor can be written as

$$C_{ijkl} = (\lambda+\mu\gamma)\delta_{ij}\delta_{kl} + \mu(1+\beta)(\delta_{ik}\delta_{jl} + \delta_{il}\delta_{jk}) + \mu(\alpha - \beta)\delta_{ijkl}\,, \tag{23}$$

where λ and μ are the Lamé constants of the elastic medium, δ_{ijkl} is unity if all the subscripts are equal and zero otherwise, and α, β, and γ depend on the lattice arrangement and elastic medium Poisson ratio σ.

The PARMECH code was used to calculate α, β, and γ for different volume fractions C and Poisson's ratio σ for the simple cubic (SC), body-centered cubic (BCC), and face-centered cubic (FCC) infinite lattices. A comparison of code results to literature values is given in Tables II-IV. The literature results are read off of small graphs and are thus not accurate at the third decimal place.

The excellent agreement of PARMECH with literature values provides confidence that the PARMECH code will predict correct results for random packs. In generating the effective elasticity tensor for these tables, a complex far field strain (i.e., $Exx = 0.03$, $Eyy = -0.06$, $Ezz = 0.1$, $Exy = 0.05$, $Exz = 0.1$, $Eyz = 0.2$) was applied to the pack in the PARMECH code simulation so that non-trivial shear and tensile stresses were applied between particles, thus ensuring that the correct solutions was not the result of the problem symmetry.

Table II. Comparison of PARMECH Results with Results of Nunan et al., (1984) and Sangani et al., (1987) for the Simple Cubic (SC) Infinite Lattice

Volume fraction C Poisson ratio σ		**α**	**β**	**γ**
C=0.4	PARMECH	2.69	1.25	0.749
σ=0.3	NK	2.71	1.27	0.744
C=0.4	PARMECH	4.43	1.29	4.73
σ=0.45	NK	4.35	1.27	4.76
C=0.47787	PARMECH	5.12	2.06	0.834
σ=0.3	NK	5.25	2.01	0.840
C=0.47787	PARMECH	9.98	2.10	5.62
σ=0.45	NK	10.4	2.01	5.67
	SL	10.0	2.10	5.53

Table III. Comparison of PARMECH Results with Results of Nunan et al., (1984) for the Face Centered Cubic (FCC) Infinite Lattice

Volume fraction *C* Poisson ratio σ		**α**	**β**	**γ**
C=0.4	PARMECH	1.32	1.66	1.46
σ=0.3	NK	1.39	na*	1.48
C=0.4	PARMECH	1.50	2.13	6.35
σ=0.45	NK	1.53	na*	6.33
C=0.6	PARMECH	3.45	4.61	3.45
σ=0.3	NK	3.48	na*	3.37
C=0.6	PARMECH	4.48	7.30	14.2
σ=0.45	NK	4.53	na*	14.1

na* Nunan-Keller results for β are incorrect according to Sangani (1987).

Table IV. Comparison of PARMECH Results with Results of Nunan et al., (1984) for the Body Centered Cubic (BCC) Infinite Lattice				
Volume fraction C Poisson ratio σ		**α**	**β**	**γ**
C=0.4	PARMECH	1.30	1.69	1.49
σ=0.3	NK	1.32	1.62	1.45
C=0.4	PARMECH	1.46	2.18	6.39
σ=0.45	NK	1.48	2.11	6.40
C=0.55	PARMECH	2.55	3.76	2.89
σ=0.3	NK	2.53	3.71	2.86
C=0.55	PARMECH	2.97	5.77	12.0
σ=0.45	NK	2.98	5.41	12.0

8.3 Random monomodal particle packs

PARMECH simulations have been performed on random particle packs with both a finite spherical geometry and infinite packs made up of repeating unit cells. Results for monomodal packs are summarized in Table V. The Poisson ratio in these calculations is 0.5. We list the order L_{max} used in the general multipole expansion and the multipole expansion for the nearest-neighbors treatment. The average minimum ε (see (22)) listed in this table is the average over all particles in the pack of the minimum ε for each particle with its closest neighbor.

The PARMECH simulations of the finite packs in Table V used a uniaxial tensile strain as described in Appendix C. The simulations of the infinite pack applied a complex far-field strain (i.e., *Exx* = 0.03, *Eyy* = -0.13, *Ezz* = 0.1, *Exy* = 0.05, *Exz* = 0.1, *Eyz* = 0.2) to the pack. The average stresses and strains in the medium were calculated as described in Appendix D for the infinite medium. For an isotropic homogeneous linear elastic medium, the average stress is

related to the average strain by

$$\bar{\tau}_{ij} = \frac{\sigma_{eff}}{1+\sigma_{eff}}(\sum_k \bar{\tau}_{kk})\delta_{ij} + 2\mu_{eff}E^a_{ij} \ .$$

The simulations were performed with the condition $\sum_k \bar{\tau}_{kk} = 0$, so that

$\bar{\tau}_{ij} = 2\mu_{eff}E^a_{ij}$ or $\mu_{eff} = \frac{\bar{\tau}_{ij}}{2E^a_{ij}}$. Because the packs do not represent a perfectly isotropic medium, we can obtain an independent effective shear modulus for each of the six independent values of *ij*. The values shown in Table V are an average of the six values with their standard deviations.

For the pack with $C = 0.06$ and $C = 0.1$, a nearest neighbors treatment is not needed and $Lmax = 8$ is adequate for good accuracy because the average minimum ε for these packs is greater than 0.1, a particle separation that was treated with good accuracy with $L_{max} = 8$ in Table I. A comparison of results with identical packs for $C = 0.3$ and $C = 0.4$ (packs with 71 and 49 particles, respectively) indicates that a maximum value of $L = 8$ for these cases is probably adequate to get the needed accuracy when the nearest-neighbors method is used. However, improved accuracy is achieved for $C = 0.5$ with $L = 12$, as seen for the pack with 50 particles.

The degree that the pack deviates from isotropy can be estimated by the standard deviation of the effective modulus. It can be seen that the packs with the higher volumes of solids have the highest deviations from isotropy. Also, as expected, the packs with larger numbers of particles generally have a lower standard deviation.

Table V. PARMECH Predictions of Effective Shear Modulus Divided by Matrix Shear Modulus (μ_{eff} / μ_{matrix}) for Monomodal Packs

Poisson's Ratio σ = 0.5

Volume fraction *C* of Pack	Pack Geometry	Average Minimum ε	L_{max}	Nearest Neighbors L_{max}	Number of Particles	μ_{eff} / μ_{matrix}
$C = 0.06$	Spherical	0.67	4	no	1279	1.18
	Spherical	0.67	4	no	12820	1.18
	Infinite	0.53	8	200	30	1.16±0.01
	Infinite	0.36	8	200	147	1.17±0.002
$C = 0.1$	Spherical	0.50	4	200	1278	1.28
	Spherical	0.50	8	200	12820	1.28
	Infinite	0.26	8	200	39	1.30±0.02
	Infinite	0.23	8	200	148	1.32±0.02
$C = 0.2$	Infinite	0.094	8	200	48	1.80±0.13
	Infinite	0.103	10	200	145	1.75±0.05
$C = 0.3$	Infinite	0.039	8	200	71	2.51±0.38
	Infinite	0.039	12	200	71	2.51±0.38
	Infinite	0.052	10	200	161	2.72±0.19
$C = 0.4$	Infinite	0.029	8	200	49	4.05±0.38
	Infinite	0.029	12	200	49	4.06±0.37
	Infinite	0.027	12	200	156	4.47±0.55
	Infinite	0.027	12	200	312	4.34±0.10
$C = 0.5$	Infinite	0.0083	8	200	50	8.66±1.15
	Infinite	0.0083	12	200	50	8.74±1.10
	Infinite	0.0121	12	200	167	7.80±2.15
	Infinite	0.0109	12	200	318	7.76±0.54
$C = 0.55$	Infinite	0.0047	12	200	47	13.28±1.09
	Infinite	0.0062	12	200	175	18.08±5.61
	Infinite	0.0071	12	200	332	12.34±1.27

8.4 Accuracy of nearest neighbors treatment

As discussed previously, the nearest-neighbors approximation treats the tensile displacements of particles in close proximity with a high order of multipole terms, and is most useful when the Poisson's ratio is close to ½. We compare the results of the code using the nearest-neighbors treatment to results obtained to high order without the nearest-neighbors approximation. Table VI shows the results of these comparisons with

monomodal particle packs at 0.50 and 0.55 volume fraction of solids. Again, the Poisson's ratio is ½.

Table VI. Comparison of Nearest Neighbors Treatment to High Order Treatment of Highly Filled Monomodal Packs
Poisson's Ratio σ = 0.5

Volume fraction C of Pack	Average Minimum ε	Number of Particles	L_{max}	Nearest Neighbors L_{max}	Memory for Matrix Storage (Gb)	Number of Iterations to Convergence	Relative CPU Time	E/E_{matrix}
C = 0.5	**0.0083**	**50**	12	200	0.85	428	1.0	8.742±1.10
			12	no	0.83	89	0.23	8.11±0.82
			16	no	1.87	121	0.56	8.43±0.92
			20	no	3.68	152	1.35	8.58±0.97
			24	no	6.54	181	2.85	8.67±1.00
			28	no	10.83	209	4.66	8.717±1.03
			32	no	16.85	234	9.13	8.744±1.04
			36	no	24.95	258	15.7	8.761±1.06
C = 0.55	**0.0047**	**47**	12	200	0.84 (in RAM)	416	1.0	13.29±1.08
			12	no	0.82 (in RAM)	97	0.41	10.59±1.71
			16	no	1.88	133	2.26	11.43±1.87
			20	no	3.75	167	5.13	11.97±1.86
			24	no	6.78	199	10.9	12.33±1.78
			28	no	11.38	233	22.1	12.57±1.68
			32	no	17.96	266	40.9	12.75±1.59
			36	no	27.17	295	65.3	12.87±1.52

From Table VI it can be seen that the nearest-neighbors treatment is effective at predicting mechanical properties of highly filled packs using a relatively low order in the multipole expansions with less memory and CPU requirements than the simulations without the nearest-neighbors option. It is also apparent that L_{max} = 12 is adequate to achieve good accuracy. We note that the predicted results with the nearest neighbors

treatment is not expected to be exactly the same as a high order multipole simulation without the nearest neighbors treatment since the nearest neighbor treatment only uses a high order multipole on the dominant tensile displacement, and does not use a higher order on the shear displacements between particles.

8.5 Random bimodal particle packs

One of the reasons the PARMECH code was developed was to help guide the construction of constitutive models that might use statistical averages for the arrangement of particles in a material to estimate its mechanical properties. Such a task can become increasingly challenging when different sizes of particles can interact in a medium. Therefore, we have run PARMECH simulations on a number of bimodal packs with particle volume fractions from 0.2 to 0.6. These have been run with the volume ratio of coarse to fine particles at 3 and 9. The ratio of diameters of coarse to fine particles varies from 2.5 to 7.5.

Results are summarized in Table VII. It will be noted that no results are given for some systems at the 0.6 volume fraction. This is because the code sometimes does not converge for high volume fractions when the nearest-neighbors treatment is used. It appears that the stiff interactions of many particles in close proximity sometimes results in particle displacements that grow during the iteration process. We have been able to improve the convergence behavior by switching on the nearest-neighbors treatment gradually, but there are still occasions when the code does not converge.

We have compared the calculations to the predictions of an effective medium theory where the large particles are assumed to be in an effective homogeneous medium

with mechanical properties of the small particles in the elastic matrix. These comparisons are shown in Table VII.

In the table the volume fraction C of the pack is given as the sum of the coarse and fine volume fractions of particles C_c and C_f. The modulus of the effective medium is calculated from a simulation of a monomodal pack at a volume fraction C_{eff} that is given by the fine particles filling a volume of the pack that consists of the total volume minus the volume of coarse particles $C_{eff} = C_f/(1 - C_c)$. The calculation of the modulus of the coarse particles was made using the same particle pack as the bimodal system, but with the fine particles removed. Clearly, when the particles sizes differ by a large amount, such an effective medium approximation should be accurate. However, when the surface-to-surface distances of the larger particles are on the order of the size of the smaller particles, then the critical high-stress region between particles cannot be treated as an effective medium. For this case, the effective medium theory should always give a larger estimate for the modulus since the region between particles is assumed to have the larger modulus of the effective medium of the fine particles. That is what is seen in these calculations. When one compares the average minimum surface-to-surface distances represented by the non-dimensional parameter ε to the particle size of the small particles, it is somewhat surprising that the effective medium theory does so well. Of coarse, the agreement is worse as the volume fraction of particles increases.

It is our plan to use these and additional calculations of the PARMECH code to assist in developing a constitutive theory based on statistical pack properties for the effective modulus of composite materials containing rigid spherical particles of different sizes.

Table VII. PARMECH (PM) Calculations of Modulus for Bimodal Particle Packs with Matrix Poisson's Ratio Equal to 1/2
Comparisons to an Effective Medium Theory (EFT)

Bimodal Pack								**Coarse Particles Alone** (Pack with fines removed)			**Effective medium, 202 fine particles**	
C_c/C_f	C	R_c/R_f	**Number of Coarse Particles**	**Number of Fine Particles**	**PM** E/E_0	**EFT** $E/E_{eff} \times E_{eff}/E_0$	**Percent Differ-ence**	C_c	**Average Minimum** ε	**PM** E/E_{eff}	C_{eff}	**PM** E_{eff}/E_0
3	0.2	2.5	54	281	1.897	1.916	1.0	0.15	0.117	1.636	0.0588	1.166
3	0.2	5.0	19	791	1.755	1.781	1.5	0.15	0.130	1.521	0.0588	1.166
3	0.2	7.5	10	1406	1.748	1.767	1.1	0.15	0.173	1.509	0.0588	1.166
3	0.4	2.5	54	281	4.700	4.562	-2.9	0.3	0.022	3.064	0.1429	1.499
3	0.4	5.0	19	791	4.074	4.203	3.2	0.3	0.045	2.823	0.1429	1.499
3	0.4	7.5	10	1406	4.547	5.127	12.7	0.3	0.019	3.443	0.1429	1.499
3	0.5	2.5	54	281	8.341	8.670	3.9	0.375	0.015	4.904	0.2	1.766
3	0.5	5.0	19	791	7.982	9.026	13.1	0.375	0.006	5.105	0.2	1.766
3	0.5	7.5	10	1406	9.489	11.122	17.2	0.375	0.010	6.291	0.2	1.766
3	0.6	2.5	54	281	nc	15.693	nc	0.45	0.006	7.012	0.2727	2.279
3	0.6	5.0	19	791	21.543	24.909	15.6	0.45	0.005	11.13	0.2727	2.279
3	0.6	7.5	10	1406	nc	17.539	nc	0.45	0.002	7.837	0.2727	2.279
9	0.2	2.5	68	118	1.888	1.874	-0.8	0.18	0.106	1.761	0.0244	1.065
9	0.2	5.0	39	542	1.761	1.770	0.5	0.18	0.134	1.664	0.0244	1.065
9	0.2	7.5	15	703	1.774	1.778	0.2	0.18	0.096	1.671	0.0244	1.065
9	0.4	2.5	68	118	4.133	4.203	1.7	0.36	0.024	3.571	0.0625	1.176
9	0.4	5.0	39	542	4.471	4.588	2.6	0.36	0.019	3.898	0.0625	1.176
9	0.4	7.5	15	703	3.834	4.015	4.7	0.36	0.028	3.411	0.0625	1.176
9	0.5	2.5	68	118	9.261	9.742	5.2	0.45	0.011	7.629	0.0909	1.269
9	0.5	5.0	39	542	6.480	6.999	8.0	0.45	0.014	5.481	0.0909	1.269
9	0.5	7.5	15	703	7.598	8.318	9.5	0.45	0.010	6.514	0.0909	1.269
9	0.6	2.5	68	118	nc	19.742	nc	0.54	0.005	13.71	0.1304	1.445
9	0.6	5.0	39	542	18.363	22.277	21.3	0.54	0.004	15.47	0.1304	1.445
9	0.6	7.5	15	703	nc	21.701	nc	0.54	0.001	15.07	0.1304	1.445

nc = no convergence

9. Summary

The PARMECH computer code calculates the stress and strain fields of a deformed medium consisting of a pack of rigid spherical particles embedded in an elastic matrix. The desired stress and strain can be calculated at any point in the medium to within a user-specified accuracy, limited only by the computation time. Average mechanical properties of the medium are also output by the code. The code can be used to simulate systems consisting of thousands of particles in a finite pack or an infinite pack consisting of a repeating rectangular cell of particles.

A multipole expansion technique is used to solve the equations of small deformation for the elastic medium and consists of truncated sums of complete orthogonal vector spherical harmonics that are exact analytical solutions for a single spherical particle. A solution is obtained by solving for the coefficients in the multipole expansion from a large set of simultaneous linear equations. Techniques are used to improve the convergence of the solution when the particles are in close proximity for highly filled mediums.

The PARMECH code results agree with exact solutions of configurations consisting of a few particles as well as infinite packs of particles in body-centered cubic, face-centered cubic, and simple cubic lattice arrangements.

The code has been used to estimate mechanical properties of a variety of monomodal and bimodal particle packs of different packing densities. Eventually, the code will be used to help derive a constitutive theory for highly filled particulate

materials with broad size distributions of particles that debond from the matrix during loading.

Appendix A. Translation coefficients of Navier multipole solutions valid on the surface of Sphere *i*

In this appendix we use addition theorems to derive off-center expansion coefficients of (11). The off-center expansion coefficient is defined as

$$C_{L_i,n_im_i}^{L_j,n_jm_j,ij} = \int_0^{2\pi} d\varphi_i \int_{-1}^{1} d(\cos\theta_i) \vec{Y}_{n_im_i}^{L_i*}(\theta_i,\varphi_i) \cdot \vec{u}_{L_j,n_jm_j}(\vec{r}-\vec{r}_j)\Big|_{|\vec{r}-\vec{r}_i|=a_i} \tag{A1}$$

where $\vec{u}_{L_j,n_jm_j}(\vec{r}-\vec{r}_j)\Big|_{|\vec{r}-\vec{r}_i|=a_i}$ is the single particle solution for sphere *j* defined in (3b) evaluated on the surface of sphere *i*. The global vector positions of the two spheres are denoted by $\vec{r}_i$ and $\vec{r}_j$. The position of Sphere *j* relative to Sphere *i* is given by $\vec{R}_{ji} = \vec{r}_j - \vec{r}_i$. We also define a vector emanating from Sphere *j* to a point on the surface of Sphere *i* by $\vec{r}_{ji} \equiv (r_{ji},\theta_{ji},\varphi_{ji}) \equiv (\vec{r}-\vec{r}_j)\Big|_{|\vec{r}-\vec{r}_i|=a}$.

The off-center expansion will consist of two parts: the harmonic term $\vec{V}_{L_j,n_jm_j}^{ex}(\vec{r}_{ji})$ and the nonharmonic term $d_{n_j}(r_{ji}^2 - a_j^2)\nabla[\nabla\cdot\vec{V}_{L_j,n_jm_j}^{ex}(\vec{r}_{ji})]$ for solutions external to the sphere. The off-center multipole expansion for the harmonic term is

$$\left(\frac{a_j}{r_{ji}}\right)^{L_j+1} \vec{Y}_{n_jm_j}^{L_j}(\theta_{ji},\varphi_{ji}) = \sum_{n_i=0}^{\infty} \sum_{L_i=n_i-1}^{n_i+1} \sum_{m_i=-n_i}^{n_i} D_{L_i;n_i,m_i}^{L_j;n_j,m_j}(\vec{R}_{ji})\ \vec{Y}_{n_im_i}^{L_i}(\theta_i,\varphi_i) \tag{A2}$$

where the expansion coefficients $D_{L_i;n_i,m_i}^{L_j;n_j,m_j}(\vec{R}_{ji})$ are functions only of the relative position vector $\vec{R}_{ji}$. We will derive them below.

The off-center multipole expansion for the nonharmonic term is

$$(2n_j-1)\sqrt{n_j(n_j+1)}\left[\left(\frac{a_j}{r_{ji}}\right)^{n_j}-\left(\frac{a_j}{r_{ji}}\right)^{n_j+2}\right]\vec{Y}^{n_j+1}_{n_jm_j}(\theta_{ji},\varphi_{ji})= \\ \sum_{n_i=0}^{\infty}\sum_{L_i=n_i-1}^{n_i+1}\sum_{m_i=-n_i}^{n_i}E^{n_j-1;n_j,m_j}_{L_i;n_i,m_i}(\vec{R}_{ji})\ \vec{Y}^{L_i}_{n_im_i}(\theta_i,\varphi_i) \tag{A3}$$

where we will only calculate the off-center term for $L_j = n_j - 1$ since the nonharmonic terms are zero for the other two values of L_j. Thus the off-center expansion coefficient is

$$C^{L_j,n_jm_j,ij}_{L_i,n_im_i}=D^{L_j;n_j,m_j}_{L_i;n_i,m_i}(\vec{R}_{ji})-\delta_{L_jn_j-1}d_{n_j}E^{n_j-1;n_j,m_j}_{L_i;n_i,m_i}(\vec{R}_{ji}) \tag{A4}$$

where d_{n_j} is the same as the d_n in (3d).

The harmonic term coefficients are given by the integral

$$D^{L_j;n_j,m_j}_{L_i;n_i,m_i}(\vec{R}_{ji})=\int_0^{2\pi}d\varphi_i\int_{-1}^{1}d(\cos\theta_i)\left(\frac{a_j}{r_{ji}}\right)^{L_j+1}\vec{Y}^{L_j}_{n_jm_j}(\theta_{ji},\varphi_{ji})\cdot\vec{Y}^{L_i*}_{n_im_i}(\theta_i,\varphi_i) \tag{A5}$$

and the nonharmonic term coefficients by the integral

$$E^{n_j-1;n_j,m_j}_{L_i;n_i,m_i}(\vec{R}_{ji})=(2n_j-1)\sqrt{n_j(n_j+1)} \\ \times\int_0^{2\pi}d\varphi_i\int_{-1}^{1}d(\cos\theta_i)\left[\left(\frac{a_j}{r_{ji}}\right)^{n_j}-\left(\frac{a_j}{r_{ji}}\right)^{n_j+2}\right]\vec{Y}^{n_j+1}_{n_jm_j}(\theta_{ji},\varphi_{ji})\cdot\vec{Y}^{L_i*}_{n_im_j}(\theta_i,\varphi_i)\quad . \tag{A6}$$

Expressions for scalar harmonic function off-center expansions, which are needed in (A5) and (A6) for the functions of $(r_{ji},\theta_{ji},\varphi_{ji})$, are given by Varshalovich (1988):

$$\frac{a_j^{L+1}}{r_{ji}^{L+1}}Y_{Lm}(\theta_{ji},\varphi_{ji})=\sqrt{\frac{4\pi(2L+1)}{(2L)!}}\sum_{\lambda=0}^{\infty}(-1)^{\lambda+m}\sqrt{\frac{(2L+2\lambda)!}{(2\lambda+1)!}}\frac{a_i^{\lambda}a_j^{L+1}}{R_{ji}^{L+\lambda+1}} \\ \times\sum_{\mu=-\lambda}^{\lambda}\begin{pmatrix}\lambda & L+\lambda & L\\ \mu & m-\mu & -m\end{pmatrix}Y_{L+\lambda,m-\mu}(\Theta_{ji},\Phi_{ji})Y_{\lambda\mu}(\theta_i,\varphi_i)\quad . \tag{A7}$$

Performing the integral of (A5) for the harmonic term of the Navier off-center expansion, one obtains

$$D_{L_i;n_i,m_i}^{L_j;n_j,m_j}(\vec{R}_{ji}) = d_{L_i;n_i,m_i}^{L_j;n_j,m_j}\frac{a_i^{L_i}a_j^{L_j+1}}{R_{ji}^{L_i+L_j+1}}Y_{L_i+L_j,m_j-m_i}(\Theta_{ji},\Phi_{ji}) \tag{A8}$$

where the constant coefficient is given by

$$\begin{aligned} d_{L_i;n_i,m_i}^{L_j;n_j,m_j} &= (-1)^{L_j+m_i}\sqrt{4\pi(2L_j+1)(2n_i+1)(2n_j+1)}\sqrt{\frac{(2L_i+2L_j)!}{(2L_i+1)!(2L_j)!}} \\ &\times\left[-\begin{pmatrix} L_i & 1 & n_i \\ m_i+1 & -1 & -m_i \end{pmatrix}\begin{pmatrix} L_i & L_i+L_j & L_j \\ m_i+1 & m_j-m_i & -m_j-1 \end{pmatrix}\begin{pmatrix} L_j & 1 & n_j \\ m_j+1 & -1 & -m_j \end{pmatrix}\right. \\ &+\begin{pmatrix} L_i & 1 & n_i \\ m_i & 0 & -m_i \end{pmatrix}\begin{pmatrix} L_i & L_i+L_j & L_j \\ m_i & m_j-m_i & -m_j \end{pmatrix}\begin{pmatrix} L_j & 1 & n_j \\ m_j & 0 & -m_j \end{pmatrix} \\ &\left.-\begin{pmatrix} L_i & 1 & n_i \\ m_i-1 & 1 & -m_i \end{pmatrix}\begin{pmatrix} L_i & L_i+L_j & L_j \\ m_i-1 & m_j-m_i & -m_j+1 \end{pmatrix}\begin{pmatrix} L_j & 1 & n_j \\ m_j-1 & 1 & -m_j \end{pmatrix}\right] \end{aligned} \tag{A9}$$

where the $\begin{pmatrix} L_1 & L_2 & L_3 \\ m_1 & m_2 & m_3 \end{pmatrix}$ are the Wigner 3j symbols which are also defined in Varshalovich (1988).

The nonharmonic term's off-center expansion is more complicated but it only exists when $L_j = n_j - 1$. We can write the nonharmonic term as follows:

$$\begin{aligned} &\left[\left(\frac{a_j}{r_{ji}}\right)^{n_j}-\left(\frac{a_j}{r_{ji}}\right)^{n_j+2}\right]\vec{Y}_{n_jm_j}^{n_j+1}(\theta_{ji},\varphi_{ji}) \\ &=\left[\left(\frac{r_{ji}}{a_j}\right)^2\left(\frac{a_j}{r_{ji}}\right)^{n_j+2}-\left(\frac{a_j}{r_{ji}}\right)^{n_j+2}\right]\vec{Y}_{n_jm_j}^{n_j+1}(\theta_{ji},\varphi_{ji}) \\ &=\frac{a_i^2+R_{ji}^2-2a_iR_{ji}\cos\alpha-a_j^2}{a_j^2}\left(\frac{a_j}{r_{ji}}\right)^{n_j+2}\vec{Y}_{n_jm_j}^{n_j+1}(\theta_{ji},\varphi_{ji}) \end{aligned} \tag{A10}$$

We have used the law of cosines, $r_{ji}^2 = a_i^2 + R_{ji}^2 - 2a_iR_{ji}\cos\alpha$, where

$$\cos\alpha = \cos\Theta_{ji}\cos\theta_i + \sin\Theta_{ji}\sin\theta_i\cos(\varphi_i - \Phi_{ji})$$
$$= \cos\Theta_{ji}\cos\theta_i + \frac{1}{2}\sin\Theta_{ji}\sin\theta_i\left(e^{i(\varphi_i-\Phi_{ji})} + e^{-i(\varphi_i-\Phi_{ji})}\right) \quad . \tag{A11}$$

Then (A6) becomes

$$E^{n_j-1;n_j,m_j}_{L_i;n_i,m_i}(\vec{R}_{ji}) = (2n_j-1)\sqrt{n_j(n_j+1)}$$
$$\times\int_0^{2\pi} d\varphi_i \int_{-1}^{1} d(\cos\theta_i)\left[\left(\frac{a_j}{r_{ji}}\right)^{n_j} - \left(\frac{a_j}{r_{ji}}\right)^{n_j+2}\right]\vec{Y}^{n_j+1}_{n_jm_j}(\theta_{ji},\varphi_{ji})\cdot\vec{Y}^{L_i*}_{n_im_i}(\theta_i,\varphi_i)$$
$$= (2n_j-1)\sqrt{n_j(n_j+1)}\int_0^{2\pi} d\varphi_i \int_{-1}^{1} d(\cos\theta_i)\left(\frac{a_j}{r_{ji}}\right)^{n_j+2}\vec{Y}^{n_j+1}_{n_jm_j}(\theta_{ji},\varphi_{ji})\cdot\vec{Y}^{L_i*}_{n_im_i}(\theta_i,\varphi_i) \tag{A12}$$
$$\times\left[\frac{a_i^2+R_{ji}^2-a_j^2}{a_j^2} - \frac{2a_iR_{ji}}{a_j^2}\cos\Theta_{ji}\cos\theta_i - \frac{a_iR_{ji}}{a_j^2}\sin\Theta_{ji}e^{-i\Phi_{ji}}\sin\theta_i e^{i\varphi_i}\right.$$
$$\left. - \frac{a_iR_{ji}}{a_j^2}\sin\Theta_{ji}e^{i\Phi_{ji}}\sin\theta_i e^{-i\varphi_i}\right]$$

The first term in the final square brackets of (A12) has no angular dependence and can be evaluated as before, *i.e.*, as a harmonic term. The second term has a $\cos\theta_i$ factor. The third term has a $\sin\theta_i e^{i\varphi_i}$ and the fourth term, a $\sin\theta_i e^{-i\varphi_i}$. The dot product of the vector spherical harmonics turns the expression into a sum of scalar spherical harmonic products. Then the second, third, and fourth terms of the final square brackets can be turned into pure spherical harmonics via the following recursion relations found again in Varshalovich (1988).

$$\cos\theta\, Y_{lm}(\theta,\varphi) = \sqrt{\frac{(l-m+1)(l+m+1)}{(2l+1)(2l+3)}}Y_{l+1,m}(\theta,\varphi)$$
$$+\sqrt{\frac{(l-m)(l+m)}{(2l-1)(2l+1)}}Y_{l-1,m}(\theta,\varphi) \tag{A13a}$$

$$\sin\theta\, e^{-i\varphi} Y_{lm}(\theta,\varphi) = \sqrt{\frac{(l-m+1)(l-m+2)}{(2l+1)(2l+3)}} Y_{l+1,m-1}(\theta,\varphi) - \sqrt{\frac{(l+m-1)(l+m)}{(2l-1)(2l+1)}} Y_{l-1,m-1}(\theta,\varphi) \tag{A13b}$$

$$\sin\theta\, e^{i\varphi} Y_{lm}(\theta,\varphi) = -\sqrt{\frac{(l+m+1)(l+m+2)}{(2l+1)(2l+3)}} Y_{l+1,m+1}(\theta,\varphi) + \sqrt{\frac{(l-m-1)(l-m)}{(2l-1)(2l+1)}} Y_{l-1,m+1}(\theta,\varphi) \tag{A13c}$$

In using these recursion relations, we note that in the integral of (A12) the vector spherical harmonic we are integrating is complex conjugated and so we use

$$\begin{aligned} \vec{Y}^{L_i *}_{n_i m_i}(\theta_i,\varphi_i)\cos\theta_i &= [\vec{Y}^{L_i}_{n_i m_i}(\theta_i,\varphi_i)\cos\theta_i]^* \\ \vec{Y}^{L_i *}_{n_i m_i}(\theta_i,\varphi_i)\sin\theta_i e^{i\varphi_i} &= [\vec{Y}^{L_i}_{n_i m_i}(\theta_i,\varphi_i)\sin\theta_i e^{-i\varphi_i}]^* \\ \vec{Y}^{L_i *}_{n_i m_i}(\theta_i,\varphi_i)\sin\theta_i e^{-i\varphi_i} &= [\vec{Y}^{L_i}_{n_i m_i}(\theta_i,\varphi_i)\sin\theta_i e^{+i\varphi_i}]^* \quad . \end{aligned} \tag{A14}$$

The entire integral of (A12) is laborious but straightforward:

$$\begin{aligned} E^{n_j-1;n_j,m_j}_{L_i;n_i,m_i}(\vec{R}_{ji}) &= (2n_j-1)\sqrt{n_j(n_j+1)}\,\frac{a_i^2+R_{ji}^2-a_j^2}{a_j^2} D^{n_j+1;n_j,m_j}_{L_i;n_i,m_i}(\vec{R}_{ji}) \\ &+ e^{n_j,m_j}_{L_i;n_i,m_i}\left(\frac{a_j}{R_{ji}}\right)^{n_j}\left(\frac{a_i}{R_{ji}}\right)^{L_i} Y_{L_i+n_j-1,m_j-m_i}(\Theta_{ji},\Phi_{ji}) \\ &+ \left(\frac{a_j}{R_{ji}}\right)^{n_j}\left[\left(\frac{a_i}{R_{ji}}\right)^{L_i} f^{n_j,m_j}_{L_i;n_i,m_i} + \left(\frac{a_i}{R_{ji}}\right)^{L_i+2} F^{n_j,m_j}_{L_i;n_i,m_i}\right] Y_{L_i+n_j+1,m_j-m_i}(\Theta_{ji},\Phi_{ji}) \\ &+ g^{n_j,m_j}_{L_i;n_i,m_i}\left(\frac{a_j}{R_{ji}}\right)^{n_j}\left(\frac{a_i}{R_{ji}}\right)^{L_i+2} Y_{L_i+n_j+3,m_j-m_i}(\Theta_{ji},\Phi_{ji}) \quad . \end{aligned} \tag{A15}$$

Detailed evaluation of $g^{n_j,m_j}_{L_i;n_i,m_i}$ shows that this coefficient is identically zero. It will not be written out explicitly in the following equations.

The coefficient $e^{n_j,m_j}_{L_i;n_i,m_i}$ of the second line of (A15) is defined by

$$e^{n_j,m_j}_{L_i;n_i,m_i} = (-1)^{n_j+m_i}\sqrt{2\pi L_i(2n_i+1)(2n_j-1)(2n_j+3)}\sqrt{\frac{(2L_i+2n_j)!}{(2L_i)!(2n_j-2)!}} \qquad \text{(A16)}$$
$$\times[\, e_1(n_j,m_j;L_i,n_i,m_i)+e_2(n_j,m_j;L_i,n_i,m_i)+e_3(n_j,m_j;L_i,n_i,m_i)\,]$$

where

$$e_1(n_j,m_j;L_i,n_i,m_i) = \left\{ \begin{pmatrix} L_i-1 & L_i+n_j & n_j+1 \\ m_i-2 & -m_i+m_j+1 & -m_j+1 \end{pmatrix} \right.$$
$$\times\sqrt{(L_i+m_i-2)(L_i+m_i-1)(L_i-m_i+n_j+m_j)(L_i-m_i+n_j+m_j+1)}$$
$$+\sqrt{(L_i-m_i+1)(L_i+m_i+n_j-m_j)}$$
$$\times\left[2\sqrt{(L_i+m_i-1)(L_i-m_i+n_j+m_j)}\begin{pmatrix} L_i-1 & L_i+n_j & n_j+1 \\ m_i-1 & -m_i+m_j & -m_j+1 \end{pmatrix} \right. \qquad \text{(A16a)}$$
$$\left.\left. +\sqrt{(L_i-m_i)(L_i+m_i+n_j-m_j+1)}\begin{pmatrix} L_i-1 & L_i+n_j & n_j+1 \\ m_i & -m_i+m_j-1 & -m_j+1 \end{pmatrix} \right] \right\}$$
$$\times\frac{\begin{pmatrix} L_i & 1 & n_i \\ m_i-1 & 1 & -m_i \end{pmatrix}\begin{pmatrix} n_j+1 & 1 & n_j \\ m_j-1 & 1 & -m_j \end{pmatrix}}{\sqrt{(2L_i-1)(2L_i+1)(2L_i+2n_j-1)(2L_i+2n_j+1)}}$$

$$e_2(n_j,m_j;L_i,n_i,m_i) = -\left\{ \begin{pmatrix} L_i-1 & L_i+n_j & n_j+1 \\ m_i-1 & -m_i+m_j+1 & -m_j \end{pmatrix} \right.$$
$$\times\sqrt{(L_i+m_i-1)(L_i+m_i)(L_i-m_i+n_j+m_j)(L_i-m_i+n_j+m_j+1)}$$
$$+\sqrt{(L_i-m_i)(L_i+m_i+n_j-m_j)}$$
$$\times\left[2\sqrt{(L_i+m_i)(L_i-m_i+n_j+m_j)}\begin{pmatrix} L_i-1 & L_i+n_j & n_j+1 \\ m_i & -m_i+m_j & -m_j \end{pmatrix} \right. \qquad \text{(A16b)}$$
$$\left.\left. +\sqrt{(L_i-m_i-1)(L_i+m_i+n_j-m_j+1)}\begin{pmatrix} L_i-1 & L_i+n_j & n_j+1 \\ m_i+1 & -m_i+m_j-1 & -m_j \end{pmatrix} \right] \right\}$$
$$\times\frac{\begin{pmatrix} L_i & 1 & n_i \\ m_i & 0 & -m_i \end{pmatrix}\begin{pmatrix} n_j+1 & 1 & n_j \\ m_j & 0 & -m_j \end{pmatrix}}{\sqrt{(2L_i-1)(2L_i+1)(2L_i+2n_j-1)(2L_i+2n_j+1)}}$$

$$e_3(n_j,m_j;L_i,n_i,m_i)=\left\{\begin{pmatrix} L_i-1 & L_i+n_j & n_j+1 \\ m_i & -m_i+m_j+1 & -m_j-1 \end{pmatrix}\right.$$
$$\times\sqrt{(L_i+m_i)(L_i+m_i+1)(L_i-m_i+n_j+m_j)(L_i-m_i+n_j+m_j+1)}$$
$$+\sqrt{(L_i-m_i-1)(L_i+m_i+n_j-m_j)}$$
$$\times\left[2\sqrt{(L_i+m_i+1)(L_i-m_i+n_j+m_j)}\begin{pmatrix} L_i-1 & L_i+n_j & n_j+1 \\ m_i+1 & -m_i+m_j & -m_j-1 \end{pmatrix}\right. \tag{A16c}$$
$$\left.\left.+\sqrt{(L_i-m_i-2)(L_i+m_i+n_j-m_j+1)}\begin{pmatrix} L_i-1 & L_i+n_j & n_j+1 \\ m_i+2 & -m_i+m_j-1 & -m_j-1 \end{pmatrix}\right]\right\}$$
$$\times\frac{\begin{pmatrix} L_i & 1 & n_i \\ m_i+1 & -1 & -m_i \end{pmatrix}\begin{pmatrix} n_j+1 & 1 & n_j \\ m_j+1 & -1 & -m_j \end{pmatrix}}{\sqrt{(2L_i-1)(2L_i+1)(2L_i+2n_j-1)(2L_i+2n_j+1)}}$$

There are two coefficients in the third line of (A15). The coefficient $f_{L_i;n_i,m_i}^{n_j,m_j}$ is given by

$$f_{L_i;n_i,m_i}^{n_j,m_j}=(-1)^{n_j+m_i+1}\sqrt{\frac{\pi\,(2n_i+1)(2n_j-1)(2n_j+3)}{(2n_j-2)!}} \tag{A17}$$
$$\times[\,f_1(n_j,m_j;L_i,n_i,m_i)+f_2(n_j,m_j;L_i,n_i,m_i)+f_3(n_j,m_j;L_i,n_i,m_i)\,]$$

where

$$f_1(n_j,m_j;L_i,n_i,m_i)=\left\{\begin{pmatrix} L_i-1 & L_i+n_j & n_j+1 \\ m_i-2 & -m_i+m_j+1 & -m_j+1 \end{pmatrix}\right.$$
$$\times\sqrt{(L_i+m_i-2)(L_i+m_i-1)(L_i+m_i+n_j-m_j)(L_i+m_i+n_j-m_j+1)}$$
$$+\sqrt{(L_i-m_i+1)(L_i-m_i+n_j+m_j+1)}$$
$$\times\left[-2\sqrt{(L_i+m_i-1)(L_i+m_i+n_j-m_j+1)}\begin{pmatrix} L_i-1 & L_i+n_j & n_j+1 \\ m_i-1 & -m_i+m_j & -m_j+1 \end{pmatrix}\right. \tag{A17a}$$
$$\left.\left.+\sqrt{(L_i-m_i)(L_i-m_i+n_j+m_j)}\begin{pmatrix} L_i-1 & L_i+n_j & n_j+1 \\ m_i & -m_i+m_j-1 & -m_j+1 \end{pmatrix}\right]\right\}$$
$$\times\frac{\sqrt{(2L_i+2n_j)!}\begin{pmatrix} L_i & 1 & n_i \\ m_i-1 & 1 & -m_i \end{pmatrix}\begin{pmatrix} n_j+1 & 1 & n_j \\ m_j-1 & 1 & -m_j \end{pmatrix}}{\sqrt{(2L_i-1)(2L_i+1)(2L_i+2n_j+1)(2L_i+2n_j+3)(2L_i-1)!}}$$

$$f_2(n_j,m_j;L_i,n_i,m_i) = -\left\{ \begin{pmatrix} L_i-1 & L_i+n_j & n_j+1 \\ m_i-1 & -m_i+m_j+1 & -m_j \end{pmatrix} \right.$$
$$\times\sqrt{(L_i+m_i-1)(L_i+m_i)(L_i+m_i+n_j-m_j)(L_i+m_i+n_j-m_j+1)}$$
$$+\sqrt{(L_i-m_i)(L_i-m_i+n_j+m_j+1)}$$
$$\times\left[-2\sqrt{(L_i+m_i)(L_i+m_i+n_j-m_j+1)}\begin{pmatrix} L_i-1 & L_i+n_j & n_j+1 \\ m_i & -m_i+m_j & -m_j \end{pmatrix}\right. \qquad \text{(A17b)}$$
$$\left.\left.+\sqrt{(L_i-m_i-1)(L_i-m_i+n_j+m_j)}\begin{pmatrix} L_i-1 & L_i+n_j & n_j+1 \\ m_i+1 & -m_i+m_j-1 & -m_j \end{pmatrix}\right]\right\}$$
$$\times\frac{\sqrt{(2L_i+2n_j)!}\begin{pmatrix} L_i & 1 & n_i \\ m_i & 0 & -m_i \end{pmatrix}\begin{pmatrix} n_j+1 & 1 & n_j \\ m_j & 0 & -m_j \end{pmatrix}}{\sqrt{(2L_i-1)(2L_i+1)(2L_i+2n_j+1)(2L_i+2n_j+3)(2L_i-1)!}}$$

$$f_3(n_j,m_j;L_i,n_i,m_i) = \left\{ \begin{pmatrix} L_i-1 & L_i+n_j & n_j+1 \\ m_i & -m_i+m_j+1 & -m_j-1 \end{pmatrix} \right.$$
$$\times\sqrt{(L_i+m_i)(L_i+m_i+1)(L_i+m_i+n_j-m_j)(L_i+m_i+n_j-m_j+1)}$$
$$+\sqrt{(L_i-m_i-1)(L_i-m_i+n_j+m_j+1)}$$
$$\times\left[-2\sqrt{(L_i+m_i+1)(L_i+m_i+n_j-m_j+1)}\begin{pmatrix} L_i-1 & L_i+n_j & n_j+1 \\ m_i+1 & -m_i+m_j & -m_j-1 \end{pmatrix}\right. \qquad \text{(A17c)}$$
$$\left.\left.+\sqrt{(L_i-m_i-2)(L_i-m_i+n_j+m_j)}\begin{pmatrix} L_i-1 & L_i+n_j & n_j+1 \\ m_i+2 & -m_i+m_j-1 & -m_j-1 \end{pmatrix}\right]\right\}$$
$$\times\frac{\sqrt{(2L_i+2n_j)!}\begin{pmatrix} L_i & 1 & n_i \\ m_i+1 & -1 & -m_i \end{pmatrix}\begin{pmatrix} n_j+1 & 1 & n_j \\ m_j+1 & -1 & -m_j \end{pmatrix}}{\sqrt{(2L_i-1)(2L_i+1)(2L_i+2n_j+1)(2L_i+2n_j+3)(2L_i-1)!}} \quad .$$

The second coefficient, $F^{n_j,m_j}_{L_i;n_i,m_i}$, in the third line of (A15) is given by

$$F^{n_j,m_j}_{L_i;n_i,m_i} = (-1)^{n_j+m_i+1}\sqrt{\frac{\pi\,(2n_i+1)(2n_j-1)(2n_j+3)}{(2n_j-2)!}} \qquad \text{(A18)}$$
$$\times[\,F_1(n_j,m_j;L_i,n_i,m_i)+F_2(n_j,m_j;L_i,n_i,m_i)+F_3(n_j,m_j;L_i,n_i,m_i)\,]$$

where

$$F_1(n_j,m_j;L_i,n_i,m_i)=\left\{\begin{pmatrix} L_i+1 & L_i+n_j+2 & n_j+1 \\ m_i-2 & -m_i+m_j+1 & -m_j+1 \end{pmatrix}\right.$$
$$\times\sqrt{(L_i-m_i+2)(L_i-m_i+3)(L_i-m_i+n_j+m_j+2)(L_i-m_i+n_j+m_j+3)}$$
$$+\sqrt{(L_i+m_i)(L_i+m_i+n_j-m_j+2)}$$
$$\times\left[-2\sqrt{(L_i-m_i+2)(L_i-m_i+n_j+m_j+2)}\begin{pmatrix} L_i+1 & L_i+n_j+2 & n_j+1 \\ m_i-1 & -m_i+m_j & -m_j+1 \end{pmatrix}\right. \tag{A18a}$$
$$\left.\left.+\sqrt{(L_i+m_i+1)(L_i+m_i+n_j-m_j+3)}\begin{pmatrix} L_i+1 & L_i+n_j+2 & n_j+1 \\ m_i & -m_i+m_j-1 & -m_j+1 \end{pmatrix}\right]\right\}$$
$$\times\frac{\sqrt{(2L_i+2n_j+4)!}\begin{pmatrix} L_i & 1 & n_i \\ m_i-1 & 1 & -m_i \end{pmatrix}\begin{pmatrix} n_j+1 & 1 & n_j \\ m_j-1 & 1 & -m_j \end{pmatrix}}{\sqrt{(2L_i+1)(2L_i+3)(2L_i+2n_j+3)(2L_i+2n_j+5)(2L_i+3)!}}$$

$$F_2(n_j,m_j;L_i,n_i,m_i)=-\left\{\begin{pmatrix} L_i+1 & L_i+n_j+2 & n_j+1 \\ m_i-1 & -m_i+m_j+1 & -m_j \end{pmatrix}\right.$$
$$\times\sqrt{(L_i-m_i+1)(L_i-m_i+2)(L_i-m_i+n_j+m_j+2)(L_i-m_i+n_j+m_j+3)}$$
$$+\sqrt{(L_i+m_i+1)(L_i+m_i+n_j-m_j+2)}$$
$$\times\left[-2\sqrt{(L_i-m_i+1)(L_i-m_i+n_j+m_j+2)}\begin{pmatrix} L_i+1 & L_i+n_j+2 & n_j+1 \\ m_i & -m_i+m_j & -m_j \end{pmatrix}\right. \tag{A18b}$$
$$\left.\left.+\sqrt{(L_i+m_i+2)(L_i+m_i+n_j-m_j+3)}\begin{pmatrix} L_i+1 & L_i+n_j+2 & n_j+1 \\ m_i+1 & -m_i+m_j-1 & -m_j \end{pmatrix}\right]\right\}$$
$$\times\frac{\sqrt{(2L_i+2n_j+4)!}\begin{pmatrix} L_i & 1 & n_i \\ m_i & 0 & -m_i \end{pmatrix}\begin{pmatrix} n_j+1 & 1 & n_j \\ m_j & 0 & -m_j \end{pmatrix}}{\sqrt{(2L_i+1)(2L_i+3)(2L_i+2n_j+3)(2L_i+2n_j+5)(2L_i+3)!}}$$

$$
\begin{aligned}
F_3(n_j,m_j;L_i,n_i,m_i) &= \left\{ \begin{pmatrix} L_i+1 & L_i+n_j+2 & n_j+1 \\ m_i & -m_i+m_j+1 & -m_j-1 \end{pmatrix} \right. \\
&\times \sqrt{(L_i-m_i)(L_i-m_i+1)(L_i-m_i+n_j+m_j+2)(L_i-m_i+n_j+m_j+3)} \\
&+ \sqrt{(L_i+m_i+2)(L_i+m_i+n_j-m_j+2)} \\
&\quad \times \left[-2\sqrt{(L_i-m_i)(L_i-m_i+n_j+m_j+2)} \begin{pmatrix} L_i+1 & L_i+n_j+2 & n_j+1 \\ m_i+1 & -m_i+m_j & -m_j-1 \end{pmatrix} \right. \\
&\quad \left. \left. + \sqrt{(L_i+m_i+3)(L_i+m_i+n_j-m_j+3)} \begin{pmatrix} L_i+1 & L_i+n_j+2 & n_j+1 \\ m_i+2 & -m_i+m_j-1 & -m_j-1 \end{pmatrix} \right] \right\} \\
&\times \frac{\sqrt{(2L_i+2n_j+4)!} \begin{pmatrix} L_i & 1 & n_i \\ m_i+1 & -1 & -m_i \end{pmatrix} \begin{pmatrix} n_j+1 & 1 & n_j \\ m_j+1 & -1 & -m_j \end{pmatrix}}{\sqrt{(2L_i+1)(2L_i+3)(2L_i+2n_j+3)(2L_i+2n_j+5)(2L_i+3)!}}
\end{aligned}
\tag{A18c}
$$

Appendix B. Treatment of a pseudo-infinite particle pack via repeating cells

A pseudo-infinite particle pack is created by making a collection of particles with centers that lie in a cubic cell with volume L^3 and then repeating the cell a large number of times in all directions. It is assumed that N_c (with $N_c >> 1$) cells from a relatively-small central portion of this pack undergo identical distortions when the whole pack is distorted. We refer to this as a pseudo-infinite pack. This geometry allows us to use the same mathematical framework as with a finite pack that has asymptotic deformations far from the particles.

The particle pack must be made so that a particle in a cell does not overlap a particle in a neighboring cell. Figure B-1 shows two adjacent cells from a two dimensional slice through a pack.

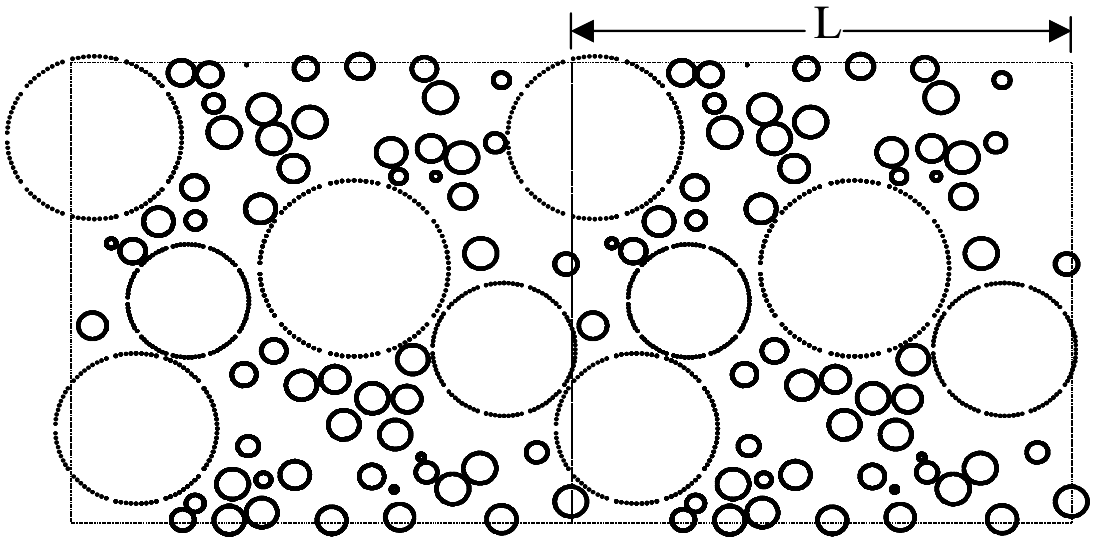

Figure B-1. Cross section of two identical adjacent cells of particles

Great computations efficiencies can be realized because only the multipole coefficients for a single cell need be stored as each cell is identical and because analytical expressions can be used to sum the effect of exterior cells on a central cell.

We delineate the cell by the subscript s with $s = 0$ being the center cell, i_s being the i^{th} particle in cell number s. Since each cell is identical, the multipole coefficients do not depend on the cell in which they are contained and $B^{i_s}_{L,nm} = B^{i}_{L,nm}$. With this nomenclature we can rewrite (11) for the particles in the center cell as

$$B^i_{L,nm} = \gamma^i_m \delta_{L0}\delta_{n1} + \psi^i_m \delta_{L1}\delta_{n1} - \sum_{n'=0}^{2}\sum_{m'=-n'}^{n'} F_{n'm'} f^{n'm',i}_{L,nm} - \sum_{s\neq 0}\sum_{L',n'm'} B^i_{L',n'm'} C^{L',n'm',i_0 i_s}_{L,nm}$$

$$- \sum_{s}\sum_{j=1,j\neq i}^{N}\sum_{L',n'm'} B^j_{L',n'm'} C^{L',n'm',i_0 j_s}_{L,nm} = \gamma^i_m \delta_{L0}\delta_{n1} + \psi^i_m \delta_{L1}\delta_{n1} - \sum_{n'=0}^{2}\sum_{m'=-n'}^{n'} F_{n'm'} f^{n'm',i}_{L,nm} \qquad \text{(B1)}$$

$$- \sum_{L',n'm'} B^i_{L',n'm'} \hat{C}^{L',n'm',ii}_{L,nm} - \sum_{j=1,j\neq i}^{N}\sum_{L',n'm'} B^j_{L',n'm'} \hat{C}^{L',n'm',ij}_{L,nm}$$

where

$$\hat{C}^{L',n'm',ii}_{L,nm} = \sum_{s\neq 0} C^{L',n'm',i_0 i_s}_{L,nm} \qquad \text{(B2a)}$$

and

$$\hat{C}^{L',n'm',ij}_{L,nm} = \sum_{s} C^{L',n'm',i_0 j_s}_{L,nm} \ . \qquad \text{(B2b)}$$

Equation (B1) is the same form as (11) with the trivial difference that the right hand side of (B1) depends on $B^i_{L,nm}$ so that the same solution technique can be applied to both the finite particle pack and the infinite particle pack of repeating cells.

To calculate the $\hat{C}^{L',n'm',ij}_{L,nm}$ one could do a direct summation over cells according to (B1). This, however, can be computationally intensive for low values of L where a large number of cells contribute. We have chosen another method. This technique will sum the effect of all particles in a cell (or some smaller portion of a cell that we will call a subcell) and, using off center expansions, will write the effect in terms of a multipole expansion centered in that cell (or subcell). The summation over all the cells can then be done a single time, saving the computational expense of summing the effect of each particle over all the cells.

We again label each cell by the subscript s. As will be shown, computational efficiencies are achieved by splitting up each cell into subcells that we enumerate with

the subscript *t* as shown in the Figure B-2. We align the boundaries of the cells so that particle *i* lies in the center of the center cell.

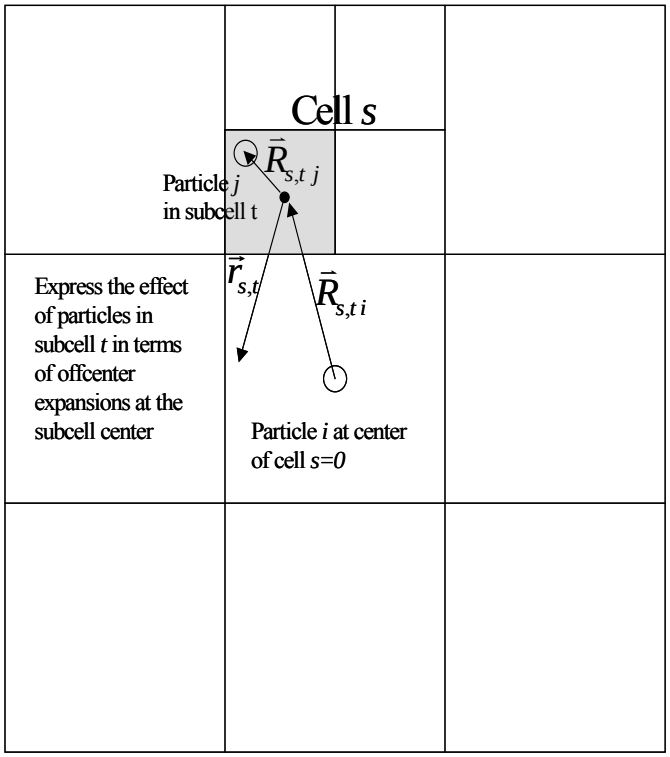

Figure B-2. The unit cell is divided into 2×2×2 = 8 subcells in the above example.

We begin the derivation by rewriting (9) for the general solution to the Navier equation with a grouping of particles in their cells and subcells as

$$\begin{aligned}\vec{u}(\vec{r}) &= \sum_{n=0}^{2}\sum_{m=-n}^{n} F_{nm} r \vec{Y}_{nm}^{1}(\theta,\varphi) + \sum_{j} \vec{u}^{\,j}(\vec{r}-\vec{R}_{j}) \\ &= \sum_{n=0}^{2}\sum_{m=-n}^{n} F_{nm} r \vec{Y}_{nm}^{1}(\theta,\varphi) + \sum_{j=1}^{N} \vec{u}^{\,j_0}(\vec{r}-\vec{R}_{j_0}) + \sum_{s\neq 0}\sum_{t=1}^{N_{sub}} \sum_{j\in \text{subcell } t} \vec{u}^{\,j_{s,t}}(\vec{r}-\vec{R}_{j_{s,t}})\end{aligned} \tag{B3}$$

where N_{sub} is the number of subcells in a cell, N_t is the number of particles contained in subcell t, and $j_{s,t}$ represents the j^{th} particle in cell s and subcell t. The second term on the

right hand side of (B3) is simply the sum of contributions from particles in the center cell and is treated in the same way as a finite pack. The last term in (B3) gives the contribution from the particles of all other cells. Its treatment is described below.

We now write the contribution of all the particles in a subcell in terms of their off-center expansion around the center of the subcell, valid for a point outside of the subcell. The appropriate off-center expansion is given in Appendix E. Using (3) and the off-center expansions we write the last term of (B3) as

$$\begin{aligned}\sum_{s\neq 0}\sum_{t=1}^{N_{sub}}\sum_{j\in\text{subcell }t}\vec{u}^{\,j_{s,t}}(\vec{r}-\vec{R}_{j_{s,t}}) &= \sum_{s\neq 0}\sum_{t=1}^{N_{sub}}\sum_{j\in\text{subcell }t}\sum_{L',n',m'}B^{j}_{L',n'm'}\vec{u}_{L',n'm'}(\vec{r}-\vec{R}_{j_{s,t}}) \\ &= \sum_{s\neq 0}\sum_{t=1}^{N_{sub}}\sum_{j\in\text{subcell }t}\sum_{L',n',m'}B^{j}_{L',n'm'} \\ &\times\left[\sum_{L'',n'',m''}\left(\widetilde{D}^{L',n'm'}_{L'',n''m''}\left(\vec{R}_{s,t\,j},r_{s,t}\right)-d_{n'}\delta_{L'n'-1}\widetilde{E}^{L',n'm'}_{L'',n''m''}\left(\vec{R}_{s,t\,j},r_{s,t}\right)\right)\vec{Y}^{L''}_{n''m''}(\theta_{s,t},\varphi_{s,t})\right]\end{aligned} \tag{B4}$$

where $\vec{R}_{s,t\,j}$ is the vector from the center of the subcell labeled by *s*,*t* to the center of particle *j* and $\vec{r}_{s,t}=\left(r_{s,t},\theta_{s,t},\varphi_{s,t}\right)$ is a vector in spherical polar coordinates centered at the center of the cell labeled by *s*,*t*.

An inspection of $\widetilde{D}^{L',n'm'}_{L'',n''m''}\left(\vec{R}_{s,t\,j},r_{s,t}\right)$ and $\widetilde{E}^{L',n'm'}_{L'',n''m''}\left(\vec{R}_{s,t\,j},r_{s,t}\right)$ in Appendix E shows that terms in (B4) are proportional to either $\frac{1}{r^{L''+1}_{s,t}}\vec{Y}^{L''}_{n''m''}(\theta_{s,t},\varphi_{s,t})$ or $\frac{1}{r^{n''}_{s,t}}\vec{Y}^{n''+1}_{n''m''}(\theta_{s,t},\varphi_{s,t})$.

Now we use off-center expansions derived in Appendix A to expand these terms at the surface of a particle *i* located at the center of the center cell (see Figure B-2).

$$\left.\frac{1}{r^{L''+1}_{s,t}}\vec{Y}^{L''}_{n''m''}(\theta_{s,t},\varphi_{s,t})\right|_{\text{Surface of }i}=\sum_{L,n,m}\overline{D}^{L'',n''m''}_{L,nm}\vec{Y}^{L}_{nm}(\theta_i,\varphi_i) \tag{B5}$$

$$\left.\frac{1}{r_{s,t}^{n''}}\vec{Y}_{n''m''}^{n''+1}(\theta_{s,t},\varphi_{s,t})\right|_{\text{Surface of } i} = \sum_{L,n,m}\overline{E}_{L,nm}^{n''-1,n''m''}\vec{Y}_{nm}^{L}(\theta_i,\varphi_i) \tag{B6}$$

where

$$\overline{D}_{L,nm}^{L'',n''m''}(\vec{R}_{s,t\,i}) = d_{L,nm}^{L'',n''m''}\frac{a_i^L}{R_{s,t\,i}^{L+L''+1}}Y_{L+L'',m''-m}(\Theta_{s,t\,i},\Phi_{s,t\,i}) \tag{B7}$$

and

$$\begin{aligned}\overline{E}_{L,nm}^{n''-1,n''m''}(\vec{R}_{s,t\,i}) &= d_{L,nm}^{n''+1,n''m''}\left(a_i^2+R_{s,t\,i}^2\right)\frac{a_i^L}{R_{s,t\,i}^{L+n''+2}}Y_{L+n''+1,m''-m}(\Theta_{s,t\,i},\Phi_{s,t\,i})\\ &+\left(2n''-1\right)\sqrt{n''\left(n''+1\right)}\left\{e_{L;n,m}^{n'',m''}\left(\frac{1}{R_{s,t\,i}}\right)^{n''}\left(\frac{a_i}{R_{s,t\,i}}\right)^{L}Y_{L+n''-1,m''-m}(\Theta_{s,t\,i},\Phi_{s,t\,i})\right.\\ &\left.+\left(\frac{1}{R_{s,t\,i}}\right)^{n''}\left[\left(\frac{a_i}{R_{s,t\,i}}\right)^{L}f_{L;n,m}^{n'',m''}+\left(\frac{a_i}{R_{s,t\,i}}\right)^{L+2}F_{L;n,m}^{n'',m''}\right]Y_{L+n''+1,m''-m}(\Theta_{s,t\,i},\Phi_{s,t\,i})\right\}\end{aligned} \tag{B8}$$

where $\vec{R}_{s,t\,i}$ is the vector from the center of particle *i* to the center of the subcell labeled by *s*,*t*. The coefficients $d_{L,nm}^{L'',n''m''}$, $e_{L,nm}^{n''m''}$, $f_{L,nm}^{n''m''}$, and $F_{L,nm}^{n''m''}$ are given in Appendix A. Substitution of (B5), (B6), (B7), and (B8) into (B4), and (B4) into (B3), yields an equation that describes the displacement field in terms of vector spherical harmonics in the reference frame of a particle *i* located at the center of the center cell. Applying the boundary condition (10) about particle *i* and the orthonormality of the vector spherical harmonics (6) yields an equation with the form of (B1) with

$$
\begin{aligned}
\hat{C}_{L,nm}^{L',n'm',ij} = & \sum_{s\neq 0}\sum_{t=1}^{N_{sub}}\sum_{L'',n'',m''}\Big[a_j^{L'+1}R_{s,t\,j}^{L''-L'}\widetilde{d}_{L'',n''m''}^{\,L',n'm'}Y_{L''-L',m'-m''}\left(\Theta_{s,t\,j},\Phi_{s,t\,j}\right) \\
& - d_{n'}\delta_{L'n'-1}(2n'-1)\sqrt{n'(n'+1)}\left(R_{s,t\,j}^2-a_j^2\right)a_j^{n'}R_{s,t\,j}^{L''-n'-1}\widetilde{d}_{L'',n''m''}^{\,n'+1,n'm'}Y_{L''-n'-1,m'-m''}\left(\Theta_{s,t\,j},\Phi_{s,t\,j}\right) \\
& - d_{n'}\delta_{L'n'-1}a_j^{n'}R_{s,t\,j}^{L''-n'+1}\widetilde{F}_{L'',n''m''}^{\,n'm'}Y_{L''-n'-1,m'-m''}\left(\Theta_{s,t\,j},\Phi_{s,t\,j}\right) \\
& - d_{n'}\delta_{L'n'-1}a_j^{n'}R_{s,t\,j}^{L''-n'+1}\widetilde{g}_{L'',n''m''}^{\,n'm'}Y_{L''-n'+1,m'-m''}\left(\Theta_{s,t\,j},\Phi_{s,t\,j}\right)\Big]\overline{D}_{L,nm}^{L'',n''m''}(\vec{R}_{s,t\,i}) \\
& + \sum_{s\neq 0}\sum_{t=1}^{N_{sub}}\sum_{n'',m''}\Big[-d_{n'}\delta_{L'n'-1}(2n'-1)\sqrt{n'(n'+1)}a_j^{n'}R_{s,t\,j}^{n''-n'}\widetilde{d}_{n''-1,n''m''}^{\,n'+1,n'm'}Y_{n''-n',m'-m''}\left(\Theta_{s,t\,j},\Phi_{s,t\,j}\right) \\
& \quad - d_{n'}\delta_{L'n'-1}a_j^{n'}R_{s,t\,j}^{n''-n'}\widetilde{f}_{n''-1,n''m''}^{\,n'm'}Y_{n''-n',m'-m''}\left(\Theta_{s,t\,j},\Phi_{s,t\,j}\right)\Big]\overline{E}_{L,nm}^{n''-1,n''m''}(\vec{R}_{s,t\,i}) \\
& + \left(1-\delta_{ij}\right)C_{L,nm}^{L',n'm',ij} + \beta_{L,nm}^{L',n'm',ij}
\end{aligned}
\tag{B9}
$$

where the second to last term in (B9) is the off-center expansion contribution of sphere *j* on sphere *i* in the center cell and $\beta_{L,nm}^{L',n'm',ij}$ is a boundary correction due to the fact that sphere *i* is not actually at the center of the center cell.

It is now evident why we split a cell into subcells for the treatment of off-center expansions. Terms in (B9) are of the form $\frac{R_{s,t\,j}^{L''}}{R_{s,t\,i}^{L''}}$ and become smaller (much less than one) as the number of subcells increase. Therefore the sum can be terminated at lower values of L'' when a cell is broken into a number of subcells.

Since (B9) depends only on the geometry of the pack, it can be evaluated a single time at the beginning of a simulation. An iterative process is used to solve for the multipole coefficients in (B1).

In the method described above, the contribution of all particles from the center cell are summed separately from the contribution of all cells other than the center cell. We have also found it efficient to sum all the particles explicitly from the 27 cells nearest the center, and then sum the contribution of all other cells. In that case, there is no need to divide the cell into subcells.

Correction due to assumption that each particle is at the center of the pack

At first glance it would appear that there could be convergence problems of the sum over cells of (B9) due to the fact that some terms in the summation for $\hat{C}_{0,1m}^{1,00,ij}$ and $\hat{C}_{0,1m}^{1,2m',ij}$ are proportional to $\frac{1}{R_{s,t\,i}^2}$ and the number of summations at a given distance increases as $R_{s,t\,i}^2$. This is not the case because the angular dependence of these terms results in cancellation of contributions from the symmetry of the cells around the central particle. However, each particle is not actually at the central point of the central collection of N_c^3 cubes. Therefore there is an additional contribution ($\beta_{L,nm}^{L',n'm',ij}$ in (B9)) for terms that are proportional to $\frac{1}{R_{s,t\,i}^2}$, because there is not a cancellation due to the symmetry of the pack. This extra term is derived below.

Let $\vec{R}_i$ be the vector from the center of the central cell to particle *i*. The center of the pack considered in (B9) is therefore shifted by $\vec{R}_i$ to the true center of the pack. When evaluating (B9) we are summing contributions from additional particles on the boundary. For example, if the *z* component of $\vec{R}_i$ is a positive $R_{z,i}$, then the boundary at a large +*z* direction contains a group of particles defined in the central cell by

$S_z^- = \{\text{particles } j, \text{ such that } R_{z,i} - R_{z,j} > L/2\}$.

The contribution from these particles must be subtracted from (B9). Similarly, the boundary at –*z* has the same group of particles removed, and their contribution must be added to (B9). We define the other groups of boundary particles as

$S_z^+ = \{\text{particles } j, \text{ such that } R_{z,j} - R_{z,i} > L/2\}$

$S_x^- = \{\text{particles } j, \text{ such that } R_{x,i} - R_{x,j} > L/2\}$

$S_x^+ = \{\text{particles } j, \text{ such that } R_{x,j} - R_{x,i} > L/2\}$

$S_y^- = \{\text{particles } j, \text{ such that } R_{y,i} - R_{y,j} > L/2\}$

$S_y^+ = \{\text{particles } j, \text{ such that } R_{y,j} - R_{y,j} > L/2\}$

where the + or – signifies whether the contributions from the particles is added or subtracted from the +boundary.

Boundary corrections only affect $\hat{C}_{0,1m}^{1,00,ij}$ and $\hat{C}_{0,1m}^{1,2m',ij}$ terms. At a distance far from the center the contribution from these particles on the boundary can be derived analytically. Far from the center, the sum over cells (cells are not broken into subcells) can be written as an integral as follows.

$$\begin{aligned}\beta_{0,1m}^{1,n'm',ij} &= -\sum_{s\in +z \text{ boundary}} C_{0,1m}^{1,n'm',i_0 j_s}\left(R_{j_s i},\Theta_{j_s i}\right)+\sum_{s\in -z \text{ boundary}} C_{0,1m}^{1,n'm',i_0 j_s}\left(R_{j_s i},\Theta_{j_s i}\right)\\ &= \frac{1}{\mathrm{L}^2}\left[-\int_{+z \text{ boundary}} dA C_{0,1m}^{1,n'm',i_0 j_s}\left(R_{j_s i},\Theta_{j_s i}\right)+\int_{-z \text{ boundary}} dA C_{0,1m}^{1,n'm',i_0 j_s}\left(R_{j_s i},\Theta_{j_s i}\right)\right]\end{aligned} \tag{B10}$$

Using the off-center expansion of Appendix A and evaluating the above integrals yields the correction for the boundaries. We do the arithmetic explicitly for the +z boundary of the evaluation of $\hat{C}_{0,1m}^{1,00,ij}$:

$$
\begin{aligned}
&\frac{1}{L^2}\int_{+z\text{ boundary}} dA\, C_{0,1m}^{1,00,i_0 j_s}\left(R_{j_s i},\Theta_{j_s i}\right)\\
&=-\frac{1}{L^2}d_{0,1m}^{1,00}\int_{-\mathrm{N_c}L/2}^{\mathrm{N_c}L/2}dx\int_{-\mathrm{N_c}L/2}^{\mathrm{N_c}L/2}dy\frac{a_j^2}{\left(\mathrm{N_c}L/2\right)^2+x^2+y^2}Y_{1,-m}\left(\arctan\left(\frac{\sqrt{x^2+y^2}}{\mathrm{N_c}L/2}\right),\arctan\left(\frac{x}{y}\right)\right)\\
&=-\frac{\delta_{0m}}{L^2}d_{0,10}^{1,00}\sqrt{\frac{3}{4\pi}}\int_{-\mathrm{N_c}L/2}^{\mathrm{N_c}L/2}dx\int_{-\mathrm{N_c}L/2}^{\mathrm{N_c}L/2}dy\frac{a_j^2\mathrm{N_c}L/2}{\left[\left(\mathrm{N_c}L/2\right)^2+x^2+y^2\right]^{\frac{3}{2}}}\\
&=-\frac{\delta_{0m}2\pi a_j^2}{3L^2}
\end{aligned}
\tag{B11}
$$

where the contributions from $C_{0,1m}^{1,00,i_0 j_s}$ and $d_{0,1m}^{1,00}$ are taken from Appendix A and the restriction to $m = 0$ is due to zero contribution from the integral for other values of m. The other integrals from (B10) can be performed similarly. Contributions from the x and y boundaries yield similar expressions. We summarize below the expressions for the boundary corrections.

$$
\begin{aligned}
\beta_{0,10}^{1,00,ij} &= -c_0 \text{ when } j\in S_z^+\\
&\quad +c_0 \text{ when } j\in S_z^-
\end{aligned}
\tag{B12a}
$$

$$
\begin{aligned}
\beta_{0,1\pm1}^{1,00,ij} &= \pm\frac{c_0}{\sqrt{2}} \text{ when } j\in S_x^+\\
&\quad \mp\frac{c_0}{\sqrt{2}} \text{ when } j\in S_x^-\\
&\quad -i\frac{c_0}{\sqrt{2}} \text{ when } j\in S_y^+\\
&\quad +i\frac{c_0}{\sqrt{2}} \text{ when } j\in S_y^-
\end{aligned}
\tag{B12b}
$$

$$\beta_{0,10}^{1,20,ij} = +c_1 \text{ when } j \in S_z^+$$
$$\quad\quad -c_1 \text{ when } j \in S_z^-$$

$$\beta_{0,1\pm1}^{1,20,ij} = \pm\frac{c_1}{2\sqrt{2}} \text{ when } j \in S_x^+ \quad \text{(B12c)}$$
$$\quad\quad \mp\frac{c_1}{2\sqrt{2}} \text{ when } j \in S_x^-$$
$$\quad\quad -\frac{c_1}{2\sqrt{2}} \text{ when } j \in S_y^+$$
$$\quad\quad +\frac{c_1}{2\sqrt{2}} \text{ when } j \in S_y^-$$

$$\beta_{0,10}^{1,2\pm1,ij} = \pm\frac{c_2}{\sqrt{2}} \text{ when } j \in S_x^+$$
$$\quad\quad \mp\frac{c_2}{\sqrt{2}} \text{ when } j \in S_x^- \quad \text{(B12d)}$$
$$\quad\quad +i\frac{c_2}{\sqrt{2}} \text{ when } j \in S_y^+$$
$$\quad\quad -i\frac{c_2}{\sqrt{2}} \text{ when } j \in S_y^-$$

$$\beta_{0,11}^{1,21,ij} = \beta_{0,1-1}^{1,2-1,ij} = -c_2 \text{ when } j \in S_z^+ \quad \text{(B12e)}$$
$$\quad\quad\quad\quad +c_2 \text{ when } j \in S_z^-$$

$$\beta_{0,1\pm1}^{1,22,ij} = -\frac{1}{4}\left(\pm\sqrt{3}c_1 - 2c_2\right)\text{when } j \in S_x^+$$
$$\quad\quad +\frac{1}{4}\left(\pm\sqrt{3}c_1 - 2c_2\right)\text{when } j \in S_x^- \quad \text{(B12f)}$$
$$\quad\quad -\frac{i}{4}\left(\sqrt{3}c_1 \mp 2c_2\right)\text{when } j \in S_y^+$$
$$\quad\quad +\frac{i}{4}\left(\sqrt{3}c_1 \mp 2c_2\right)\text{when } j \in S_y^-$$

$$\begin{aligned}\beta_{0,1\pm1}^{1,2-2,ij} &= -\frac{1}{4}\left(\pm\sqrt{3}c_1 + 2c_2\right)\text{when } j \in S_x^+ \\ &+ \frac{1}{4}\left(\pm\sqrt{3}c_1 + 2c_2\right)\text{when } j \in S_x^- \\ &- \frac{i}{4}\left(\sqrt{3}c_1 \pm 2c_2\right)\text{when } j \in S_y^+ \\ &+ \frac{i}{4}\left(\sqrt{3}c_1 \pm 2c_2\right)\text{when } j \in S_y^-\end{aligned} \tag{B12g}$$

with

$$\begin{aligned}c_0 &= \frac{4\pi a_j^2}{3L^2} \\ c_1 &= \frac{a_j^2}{L^2}\left[\frac{10\sqrt{2}\pi(1-2\sigma)}{3(4-5\sigma)} + \frac{5\sqrt{6}}{(4-5\sigma)}\right] \\ c_2 &= \frac{a_j^2}{L^2}\left[\frac{5\sqrt{2}}{(4-5\sigma)} - \frac{10\sqrt{\frac{2}{3}}\pi(1-\sigma)}{(4-5\sigma)}\right]\end{aligned} \tag{B13}$$

All other $\beta_{L,nm}^{L',n'm',ij}$ are zero.

Appendix C. Mechanical properties for a particle pack of spherical geometry

The mechanical properties of a spherical pack of particles can be estimated from the exact solution of an isolated spherical elastic body of radius *a* with shear modulus μ_e and Poisson's ratio σ_e embedded in a uniform elastic medium with shear modulus μ and Poisson's ratio σ (Goodier, 1933). For uniaxial tensile displacement with strain E_{zz}, we can compare the exact Goodier solution to the multipole solution to order $\frac{1}{r^2}$ (*r* is the distance from the sphere center) to relate the mechanical properties of the embedded sphere to the multipole moments. In spherical coordinates and to order $\frac{1}{r^2}$, the Goodier solution for displacement in the region far from the sphere is given by

$$u_r = -\frac{A}{r^2} + \frac{C(5-4\sigma)}{(1-2\sigma)r^2}\cos(2\theta) \tag{C1a}$$

$$u_\theta = -\frac{2C}{r^2}\sin(2\theta), \tag{C1b}$$

where

$$A = \frac{E_{zz}(1+\sigma)a^3}{4}\left[-\frac{\mu-\mu_e}{(7-5\sigma)\mu+(8-10\sigma)\mu_e}\frac{(1-2\sigma_e)(6-5\sigma)2\mu+(3+19\sigma_e-20\sigma\sigma_e)\mu_e}{(1-2\sigma_e)2\mu+(1+\sigma_e)\mu_e} \right.$$
$$\left. +2\frac{\left((1-\sigma)\frac{1+\sigma_e}{1+\sigma}-\sigma_e\right)\mu_e-(1-2\sigma_e)\mu}{(1-2\sigma_e)2\mu+(1+\sigma_e)\mu_e} \right]$$

$$C = \frac{E_{zz}(1+\sigma)a^3}{4}\frac{5(1-2\sigma)(\mu-\mu_e)}{(7-5\sigma)\mu+(8-10\sigma)\mu_e}.$$

The multipole solution for the pack can be written to the same order in r using (3) and (9) for the displacement field. Because the $B^i_{0,1m}$ and $B^i_{1,1m}$ are zero for a pack in equilibrium (i.e., forces and torques on each particle are zero), the only terms that contribute to $\frac{1}{r^2}$ are the $B^i_{1,00}$ and $B^i_{1,2m}$ coefficients. Only the $m = 0$ term contributes in $B^i_{1,2m}$ for a large random pack since the $m \neq 0$ terms imply that there is not azimuthal symmetry. Keeping only these terms it is a simple exercise to write (3) and (9) in the form of (C1). In terms of the multipole coefficients the constants A and C are

$$A = \frac{1}{\sqrt{4\pi}}\sum_i a_i^2 B^i_{1,00} - \frac{5(5-4\sigma)}{16\sqrt{2\pi}(4-5\sigma)}\sum_i a_i^2 B^i_{1,20} \tag{C2}$$

$$C = \frac{15(1-2\sigma)}{16\sqrt{2\pi}(4-5\sigma)}\sum_i a_i^2 B^i_{1,20} \tag{C3}$$

By equating A and C in (C1), (C2), and (C3), one can solve for the effective mechanical properties of the spherical pack of particles in terms of the multipole coefficients and the mechanical properties of the binder matrix.

$$\mu_e = \frac{1 - \frac{(7-5\sigma)}{(8-10\sigma)} F}{1+F} \mu \tag{C4a}$$

$$\sigma_e = \frac{G(2\mu + \mu_e) + (1+\sigma)\mu - (1-2\sigma)\mu_e}{G(4\mu - \mu_e) + 2(1+\sigma)\mu + (1-2\sigma)\mu_e} \tag{C4b}$$

$$F = \frac{3\sum_i a_i^2 B_{1,20}^i}{E_{zz} 2\sqrt{2\pi}(1+\sigma)a^3}$$

$$G = \frac{3\sum_i a_i^2 B_{1,00}^i}{E_{zz}\sqrt{4\pi}\, a^3}.$$

APPENDIX D. Mechanical properties for an infinite pack

In this appendix we derive the equations that allow the mechanical properties for an infinite pack to be calculated from the coefficients of the multipole expansion. We do not limit this derivation to isotropic packs. In general the effective mechanical properties of a medium can be derived from the average stresses and strains in that medium. For a material made up of rigid particles embedded in an elastic matrix, the average stress $\bar{\tau}_{ij}$ (*i*,*j* indices range over *x*, *y*, and *z* values) in the material is given by the average of the sum of stresses in the particles and the binder as

$$\bar{\tau}_{ij} = \frac{1}{V}\int \tau_{ij} dV = \frac{1}{V}\sum_p I_{ij}^p + B_{ij} \tag{D1}$$

where

$$I_{ij}^{p} = \int_{Particle\ p} \tau_{ij} dV \quad \text{and} \quad B_{ij} = \frac{1}{V} \int_{Binder} \tau_{ij} dV \,. \tag{D2}$$

The volume of the system under consideration is V. For void-free material B_{ij} is related to the average strain $\boldsymbol{E}^{a}$ induced in the medium by

$$B_{ij} = \lambda\left(E_{xx}^{a} + E_{yy}^{a} + E_{zz}^{a}\right)\delta_{ij} + 2\mu(E_{ij}^{a}) \tag{D3}$$

where λ and μ are the Lamé constants of the binder.

To evaluate the average stress in the material we must separately evaluate the contributions from the particles and binder as in (D1). The contribution for the average stress in the particles is derived next.

Equation (D2) for the volume integral of τ_{ij} in particle p can be turned into a surface integral as (iz component shown):

$$\begin{aligned} I_{iz}^{p} &= \int_{Particle\ p} \tau_{iz} dV = \int_{Particle\ p} \tau_{iz} dxdydz = \int_{-a_p}^{a_p} dz \int_{\text{Surface } S_1} \tau_{iz} dxdy \\ &= \int_{-a_p}^{a_p} dz \int_{\text{Surface } S_1} \hat{n}_i \cdot \boldsymbol{\tau} \cdot d\vec{a} = \int_{-a_p}^{a_p} dz \int_{\text{Surface } S_2} \hat{n}_i \cdot \boldsymbol{\tau} \cdot d\vec{a} \end{aligned} \tag{D4}$$

where the surface S_1 is the plane surface inside the sphere perpendicular to the z axis and passing through z, S_2 is the surface of the sphere for all points greater than z, and a_p is the radius of particle p. The identity on the right hand side of (D4) is derived from the equation $\nabla \cdot \boldsymbol{\tau} = 0$ for a body in equilibrium and Gauss's theorem (with signs adjusted to the orientation of $d\vec{a}$).

$$0 = \int_{\substack{\text{Volume bounded} \\ \text{by } S_1+S_2}} \hat{n}_i \cdot \boldsymbol{\tau} \cdot \bar{\nabla} dV = \int_{\substack{\text{Surface} \\ S_1+S_2}} \hat{n}_i \cdot \boldsymbol{\tau} \cdot d\vec{a} = \int_{\text{Surface } S_1} \hat{n}_i \cdot \boldsymbol{\tau} \cdot d\vec{a} + \int_{\text{Surface } S_2} \hat{n}_i \cdot \boldsymbol{\tau} \cdot d\vec{a} \tag{D5}$$

Equation (D4) can be simplified by switching the order of the z and surface integrals, and performing the z integral explicitly. The result is

$$I_{iz}^{p} = \int_{\text{Particle } p} \tau_{iz} dV = \int_{\substack{\text{Surface of} \\ \text{Particle p}}} z\, \hat{n}_i \cdot \boldsymbol{\tau} \cdot d\vec{a} \tag{D6a}$$

where z is the distance in the z direction from the center of the particle to the position of the surface element $d\vec{a}$. Similarly,

$$I_{ix}^{p} = \int_{\substack{\text{Surface of} \\ \text{Particle p}}} x\, \hat{n}_i \cdot \boldsymbol{\tau} \cdot d\vec{a} \tag{D6b}$$

and

$$I_{iy}^{p} = \int_{\substack{\text{Surface of} \\ \text{Particle p}}} y\, \hat{n}_i \cdot \boldsymbol{\tau} \cdot d\vec{a}\,. \tag{D6c}$$

It is now a straightforward, if tedious, exercise to calculate the I_{ij}^{p} in terms of the coefficients $B_{L,nm}^{p}$ of the multipole expansion. The stress is calculated from the general multipole solution for the displacement field, and then substituted into (D6). The results for the volume integral of stresses in the particles are as follows.

$$I_{zz}^{p} = \mu 4\sqrt{\pi}\left[\frac{1-\sigma}{1-2\sigma}\sum_{p} a_p^2 B_{1,00}^{p} - \frac{5(1-\sigma)}{\sqrt{2}(4-5\sigma)}\sum_{p} a_p^2 B_{1,20}^{p}\right] \tag{D7a}$$

$$I_{xx}^{p} = \mu 4\sqrt{\pi}\left[\frac{1-\sigma}{1-2\sigma}\sum_{p} a_p^2 B_{1,00}^{p} + \frac{5(1-\sigma)}{2\sqrt{2}(4-5\sigma)}\sum_{p} a_p^2\left[B_{1,20}^{p} - \sqrt{\tfrac{3}{2}}\left(B_{1,22}^{p} + B_{1,2-2}^{p}\right)\right]\right] \tag{D7b}$$

$$I_{yy}^{p} = \mu 4\sqrt{\pi}\left[\frac{1-\sigma}{1-2\sigma}\sum_{p} a_p^2 B_{1,00}^{p} + \frac{5(1-\sigma)}{2\sqrt{2}(4-5\sigma)}\sum_{p} a_p^2\left[B_{1,20}^{p} + \sqrt{\tfrac{3}{2}}\left(B_{1,22}^{p} + B_{1,2-2}^{p}\right)\right]\right] \tag{D7c}$$

$$I_{zx}^{p} = I_{xz}^{p} = \mu 5\sqrt{3\pi}\,\frac{(1-\sigma)}{(4-5\sigma)}\sum_{p} a_p^2\left(B_{1,21}^{p} - B_{1,2-1}^{p}\right) \tag{D7d}$$

$$I_{zy}^{p} = I_{yz}^{p} = i\mu 5\sqrt{3\pi}\,\frac{(1-\sigma)}{(4-5\sigma)}\sum_{p} a_p^2\left(B_{1,21}^{p} + B_{1,2-1}^{p}\right) \tag{D7e}$$

$$I_{yx}^{p} = I_{xy}^{p} = i\mu 5\sqrt{3\pi}\,\frac{(1-\sigma)}{(4-5\sigma)}\sum_{p} a_p^2\left(B_{1,2-2}^{p} - B_{1,22}^{p}\right) \tag{D7f}$$

We next evaluate the average stress in the binder using (D3). To do this we must calculate the average strain $\mathbf{E^a}$ in the material. The average *zz* component of strain is given by the change in the $\pm z$ wall position of the unit cell divided by its length as

$$\begin{aligned} E^a_{zz} &= \left(u_z(x,y,z+L) - u_z(x,y,z)\right)/L \\ &= E^{\inf}_{zz} + \frac{1}{L}\sum_{L'n'm'}\sum_p B^{\mathrm{p}}_{L',n'm'}\beta^{L'n'm'}_{010}\Big|_{\text{z boundary}}\left|\vec{Y}^0_{10}\right| \\ &= E^{\inf}_{zz} + \frac{1}{L\sqrt{4\pi}}\sum_{L'n'm'}\sum_p B^{\mathrm{p}}_{L',n'm'}\beta^{L'n'm'}_{010}\Big|_{\text{z boundary}} \\ &= E^{\inf}_{zz} - \frac{\sqrt{4\pi}}{3L^3}\sum_p B^{\mathrm{p}}_{1,00}a_p^2 + \frac{1}{L^3}\left(\frac{5\sqrt{2\pi}(1-2\sigma)}{3(4-5\sigma)} + \frac{5\sqrt{\frac{3}{2\pi}}}{(4-5\sigma)}\right)\sum_p B^{\mathrm{p}}_{1,20}a_p^2 \end{aligned} \tag{D8a}$$

where the contributions to the difference of the displacement over a periodic cell come only from the far field strain at infinity $E^{\inf}_{zz}$ and the boundary corrections (equations (B12) and (B13)) derived in Appendix B. Similarly, it can be shown that the other components of average strain are given by

$$\begin{aligned} E^a_{xx} = E^{\inf}_{xx} &- \frac{\sqrt{4\pi}}{3L^3}\sum_p B^{\mathrm{p}}_{1,00}a_p^2 - \\ &\frac{1}{2L^3}\left(\frac{5\sqrt{2\pi}(1-2\sigma)}{3(4-5\sigma)} + \frac{5\sqrt{\frac{3}{2\pi}}}{(4-5\sigma)}\right)\left[\sum_p a_p^2\left[B^p_{1,20} - \sqrt{\tfrac{3}{2}}\left(B^p_{1,22} + B^p_{1,2-2}\right)\right]\right] \end{aligned} \tag{D8b}$$

$$\begin{aligned} E^a_{yy} = E^{\inf}_{yy} &- \frac{\sqrt{4\pi}}{3L^3}\sum_p B^{\mathrm{p}}_{1,00}a_p^2 - \\ &\frac{1}{2L^3}\left(\frac{5\sqrt{2\pi}(1-2\sigma)}{3(4-5\sigma)} + \frac{5\sqrt{\frac{3}{2\pi}}}{(4-5\sigma)}\right)\left[\sum_p a_p^2\left[B^p_{1,20} + \sqrt{\tfrac{3}{2}}\left(B^p_{1,22} + B^p_{1,2-2}\right)\right]\right] \end{aligned} \tag{D8c}$$

$$E^a_{zx} = E^a_{xz} = E^{\inf}_{xz} + \frac{1}{\mathrm{L}^3}\left(\frac{5}{2\sqrt{\pi}(4-5\sigma)} - \frac{5\sqrt{\frac{\pi}{3}}(1-\sigma)}{(4-5\sigma)}\right)\sum_p a_p^2\left(B^p_{1,21} - B^p_{1,2-1}\right) \tag{D8d}$$

$$E^a_{zy} = E^a_{yz} = E^{\inf}_{yz} + \frac{\mathrm{i}}{\mathrm{L}^3}\left(\frac{5}{2\sqrt{\pi}(4-5\sigma)} - \frac{5\sqrt{\frac{\pi}{3}}(1-\sigma)}{(4-5\sigma)}\right)\sum_p a_p^2\left(B^p_{1,21} + B^p_{1,2-1}\right) \tag{D8e}$$

$$E_{yx}^{a} = E_{xy}^{a} = E_{xy}^{\inf} + \frac{\mathrm{i}}{\mathrm{L}^3}\left(\frac{5}{2\sqrt{\pi}(4-5\sigma)} - \frac{5\sqrt{\frac{\pi}{3}}(1-\sigma)}{(4-5\sigma)}\right)\sum_{p} a_p^2\left(B_{1,2-2}^{p} - B_{1,22}^{p}\right) \qquad \text{(D8f)}$$

Equations A-6.5 and A-6.6 can be substituted into equations A-6.1 through A-6.3 to calculate the average stress tensor in the medium from the coefficients of the multipole expansion. Using the average strain tensor calculated in eq. A-6.6 then allows the mechanical properties of the medium to be extracted.

Appendix E. Translation coefficients of Navier multipole solutions valid far from the surface of sphere *i*

In Appendix A off-center expansions were derived for the multipole solution of sphere *j* on the surface of sphere *i* in a reference frame centered at *i*. A different set of expansions is needed for points far from the surface of sphere *i*. These expansions are valid when the distance r_i from sphere *i* is greater than the separation R_{ji} between spheres *i* and *j*. The derivation is very similar to that presented Appendix A. For brevity, we present only the results. The nomenclature remains the same, with the exception of the definition of $\vec{r}_{ji}$ which is defined as

$$\vec{r}_{ji} = \vec{r}_i - \vec{R}_{ji} \ . \qquad \text{(E1)}$$

The off-center multipole expansion for the harmonic term is

$$\left(\frac{a_j}{r_{ji}}\right)^{L_j+1} \vec{Y}_{n_j m_j}^{L_j}(\theta_{ji}, \varphi_{ji}) = \sum_{n_i=0}^{\infty} \sum_{L_i=n_i-1}^{n_i+1} \sum_{m_i=-n_i}^{n_i} \widetilde{D}_{L_i;n_i,m_i}^{L_j;n_j,m_j}(\vec{R}_{ji}, r_i)\ \vec{Y}_{n_i m_i}^{L_i}(\theta_i, \varphi_i) \qquad \text{(E2)}$$

where the expansion coefficients $\widetilde{D}_{L_i;n_i,m_i}^{L_j;n_j,m_j}(\vec{R}_{ji}, r_i)$ are functions only of the relative position vector $\vec{R}_{ji}$ and the distance r_i from sphere *i*.

The off-center multipole expansion for the nonharmonic term is

$$(2n_j-1)\sqrt{n_j(n_j+1)}\left[\left(\frac{a_j}{r_{ji}}\right)^{n_j}-\left(\frac{a_j}{r_{ji}}\right)^{n_j+2}\right]\vec{Y}^{n_j+1}_{n_jm_j}(\theta_{ji},\varphi_{ji})$$
$$=\sum_{n_i=0}^{\infty}\sum_{L_i=n_i-1}^{n_i+1}\sum_{m_i=-n_i}^{n_i}\widetilde{E}^{n_j-1;n_j,m_j}_{L_i;n_i,m_i}(\vec{R}_{ji},r_i)\;\vec{Y}^{L_i}_{n_im_i}(\theta_i,\varphi_i) \tag{E3}$$

where we will only calculate the off-center term for $L_j = n_j - 1$ since the nonharmonic terms are zero for the other two values of L_j.

The harmonic term coefficients are given by the integral

$$\widetilde{D}^{L_j;n_j,m_j}_{L_i;n_i,m_i}(\vec{R}_{ji},r_i)=\int_0^{2\pi}d\varphi_i\int_{-1}^{1}d(\cos\theta_i)\left(\frac{a_j}{r_{ji}}\right)^{L_j+1}\vec{Y}^{L_j}_{n_jm_j}(\theta_{ji},\varphi_{ji})\cdot\vec{Y}^{L_i*}_{n_im_i}(\theta_i,\varphi_i) \tag{E4}$$

and the nonharmonic term coefficients by the integral

$$\widetilde{E}^{n_j-1;n_j,m_j}_{L_i;n_i,m_i}(\vec{R}_{ji},r_i)=(2n_j-1)\sqrt{n_j(n_j+1)}$$
$$\times\int_0^{2\pi}d\varphi_i\int_{-1}^{1}d(\cos\theta_i)\left[\left(\frac{a_j}{r_{ji}}\right)^{n_j}-\left(\frac{a_j}{r_{ji}}\right)^{n_j+2}\right]\vec{Y}^{n_j+1}_{n_jm_j}(\theta_{ji},\varphi_{ji})\cdot\vec{Y}^{L_i*}_{n_im_i}(\theta_i,\varphi_i)\,. \tag{E5}$$

Expressions for scalar harmonic function off-center expansions, which are needed in (E4) and (E5) for the functions of $(r_{ji},\theta_{ji},\varphi_{ji})$, are given by Varshalovich (1988):

$$\frac{a_j^{L+1}}{r_{ji}^{L+1}}Y_{Lm}(\theta_{ji},\varphi_{ji})=\sqrt{\frac{4\pi(2L+1)}{(2L)!}}\sum_{\lambda=L}^{\infty}(-1)^{\lambda+m}\sqrt{\frac{(2\lambda)!}{(2(\lambda-L)+1)!}}\frac{a_j^{L+1}R_{ji}^{\lambda-L}}{r_i^{\lambda+1}}$$
$$\times\sum_{\mu=-\lambda}^{\lambda}\begin{pmatrix}\lambda & \lambda-L & L\\ \mu & m-\mu & -m\end{pmatrix}Y_{\lambda-L,m-\mu}(\Theta_{ji},\Phi_{ji})Y_{\lambda\mu}(\theta_i,\varphi_i)\,. \tag{E6}$$

Performing the integral of (E4) for the harmonic term of the Navier off-center expansion, one obtains

$$\widetilde{D}^{L_j;n_j,m_j}_{L_i;n_i,m_i}(\vec{R}_{ji},r_i)=\widetilde{d}^{L_j;n_j,m_j}_{L_i;n_i,m_i}\frac{a_j^{L_j+1}R_{ji}^{L_i-L_j}}{r_i^{L_i+1}}Y_{L_i-L_j,m_j-m_i}(\Theta_{ji},\Phi_{ji}) \tag{E7}$$

where the constant coefficient is given by

$$\widetilde{d}^{L_j;n_j,m_j}_{L_i;n_i,m_i} = (-1)^{L_j+m_i}\sqrt{4\pi(2L_j+1)(2n_i+1)(2n_j+1)}\sqrt{\frac{(2L_i)!}{\big(2(L_i-L_j)+1\big)!(2L_j)!}}$$
$$\times\Bigg[-\begin{pmatrix} L_i & 1 & n_i \\ m_i+1 & -1 & -m_i \end{pmatrix}\begin{pmatrix} L_i & L_i-L_j & L_j \\ m_i+1 & m_j-m_i & -m_j-1 \end{pmatrix}\begin{pmatrix} L_j & 1 & n_j \\ m_j+1 & -1 & -m_j \end{pmatrix}$$
$$+\begin{pmatrix} L_i & 1 & n_i \\ m_i & 0 & -m_i \end{pmatrix}\begin{pmatrix} L_i & L_i-L_j & L_j \\ m_i & m_j-m_i & -m_j \end{pmatrix}\begin{pmatrix} L_j & 1 & n_j \\ m_j & 0 & -m_j \end{pmatrix} \tag{E8}$$
$$-\begin{pmatrix} L_i & 1 & n_i \\ m_i-1 & 1 & -m_i \end{pmatrix}\begin{pmatrix} L_i & L_i-L_j & L_j \\ m_i-1 & m_j-m_i & -m_j+1 \end{pmatrix}\begin{pmatrix} L_j & 1 & n_j \\ m_j-1 & 1 & -m_j \end{pmatrix}\Bigg] \quad .$$

The nonharmonic term's off-center expansion is as follows:

$$\widetilde{E}^{n_j-1;n_j,m_j}_{L_i;n_i,m_i}(\vec{R}_{ji},r_i) = (2n_j-1)\sqrt{n_j(n_j+1)}\,\frac{r_i^2+R_{ji}^2-a_j^2}{a_j^2}\,\widetilde{D}^{n_j+1;n_j,m_j}_{L_i;n_i,m_i}(\vec{R}_{ji},r_i)$$
$$+\widetilde{e}^{n_j,m_j}_{L_i;n_i,m_i}\left(\frac{a_j}{R_{ji}}\right)^{n_j}\left(\frac{R_{ji}}{r_i}\right)^{L_i-1}Y_{L_i-n_j-3,m_j-m_i}(\Theta_{ji},\Phi_{ji})$$
$$+\left(\frac{a_j}{R_{ji}}\right)^{n_j}\left[\left(\frac{R_{ji}}{r_i}\right)^{L_i-1}\widetilde{f}^{n_j,m_j}_{L_i;n_i,m_i}+\left(\frac{R_{ji}}{r_i}\right)^{L_i+1}\widetilde{F}^{n_j,m_j}_{L_i;n_i,m_i}\right]Y_{L_i-n_j-1,m_j-m_i}(\Theta_{ji},\Phi_{ji}) \tag{E9}$$
$$+\widetilde{g}^{n_j,m_j}_{L_i;n_i,m_i}\left(\frac{a_j}{R_{ji}}\right)^{n_j}\left(\frac{R_{ji}}{r_i}\right)^{L_i+1}Y_{L_i-n_j+1,m_j-m_i}(\Theta_{ji},\Phi_{ji}) \quad .$$

Detailed evaluation shows that the coefficient $\widetilde{e}^{n_j,m_j}_{L_i;n_i,m_i}$ is always zero. It will not be written out explicitly.

The coefficient $\widetilde{f}^{n_j,m_j}_{L_i;n_i,m_i}$ is given by

$$\widetilde{f}^{n_j,m_j}_{L_i;n_i,m_i} = (-1)^{n_j+m_i+1}\sqrt{\frac{\pi\,(2n_i+1)(2n_j-1)(2n_j+3)}{(2n_j-2)!}} \tag{E10}$$
$$\times[\,\widetilde{f}_1(n_j,m_j;L_i,n_i,m_i)+\widetilde{f}_2(n_j,m_j;L_i,n_i,m_i)+\widetilde{f}_3(n_j,m_j;L_i,n_i,m_i)]$$

where

$$\widetilde{f}_1(n_j,m_j;L_i,n_i,m_i)=\left\{\begin{pmatrix} L_i-1 & L_i-n_j-2 & n_j+1 \\ m_i-2 & -m_i+m_j+1 & -m_j+1 \end{pmatrix}\right.$$
$$\times\sqrt{(L_i+m_i-2)(L_i+m_i-1)(L_i+m_i-n_j-m_j-2)(L_i+m_i-n_j-m_j-1)}$$
$$+\sqrt{(L_i-m_i+1)(L_i-m_i-n_j+m_j-1)}$$
$$\times\left[-2\sqrt{(L_i+m_i-1)(L_i+m_i-n_j-m_j-1)}\begin{pmatrix} L_i-1 & L_i-n_j-2 & n_j+1 \\ m_i-1 & -m_i+m_j & -m_j+1 \end{pmatrix}\right. \qquad \text{(E10a)}$$
$$\left.\left.+\sqrt{(L_i-m_i)(L_i-m_i-n_j+m_j-2)}\begin{pmatrix} L_i-1 & L_i-n_j-2 & n_j+1 \\ m_i & -m_i+m_j-1 & -m_j+1 \end{pmatrix}\right]\right\}$$
$$\times\frac{\sqrt{(2L_i-2)!}\begin{pmatrix} L_i & 1 & n_i \\ m_i-1 & 1 & -m_i \end{pmatrix}\begin{pmatrix} n_j+1 & 1 & n_j \\ m_j-1 & 1 & -m_j \end{pmatrix}}{\sqrt{(2L_i-1)(2L_i+1)(2L_i-2n_j-3)(2L_i-2n_j-1)(2L_i-2n_j-3)!}}$$

$$\widetilde{f}_2(n_j,m_j;L_i,n_i,m_i)=-\left\{\begin{pmatrix} L_i-1 & L_i-n_j-2 & n_j+1 \\ m_i-1 & -m_i+m_j+1 & -m_j \end{pmatrix}\right.$$
$$\times\sqrt{(L_i+m_i-1)(L_i+m_i)(L_i+m_i-n_j-m_j-2)(L_i+m_i-n_j-m_j-1)}$$
$$+\sqrt{(L_i-m_i)(L_i-m_i-n_j+m_j-1)}$$
$$\times\left[-2\sqrt{(L_i+m_i)(L_i+m_i-n_j-m_j-1)}\begin{pmatrix} L_i-1 & L_i-n_j-2 & n_j+1 \\ m_i & -m_i+m_j & -m_j \end{pmatrix}\right. \qquad \text{(E10b)}$$
$$\left.\left.+\sqrt{(L_i-m_i-1)(L_i-m_i-n_j+m_j-2)}\begin{pmatrix} L_i-1 & L_i-n_j-2 & n_j+1 \\ m_i+1 & -m_i+m_j-1 & -m_j \end{pmatrix}\right]\right\}$$
$$\times\frac{\sqrt{(2L_i-2)!}\begin{pmatrix} L_i & 1 & n_i \\ m_i-1 & 1 & -m_i \end{pmatrix}\begin{pmatrix} n_j+1 & 1 & n_j \\ m_j-1 & 1 & -m_j \end{pmatrix}}{\sqrt{(2L_i-1)(2L_i+1)(2L_i-2n_j-3)(2L_i-2n_j-1)(2L_i-2n_j-3)!}}$$

$$\widetilde{f}_3(n_j,m_j;L_i,n_i,m_i)=\left\{\begin{pmatrix} L_i-1 & L_i-n_j-2 & n_j+1 \\ m_i & -m_i+m_j+1 & -m_j-1 \end{pmatrix}\right.$$
$$\times\sqrt{(L_i+m_i)(L_i+m_i+1)(L_i+m_i-n_j-m_j-2)(L_i+m_i-n_j-m_j-1)}$$
$$+\sqrt{(L_i-m_i-1)(L_i-m_i-n_j+m_j-1)}$$
$$\times\left[-2\sqrt{(L_i+m_i+1)(L_i+m_i-n_j-m_j-1)}\begin{pmatrix} L_i-1 & L_i-n_j-2 & n_j+1 \\ m_i+1 & -m_i+m_j & -m_j-1 \end{pmatrix}\right. \tag{E10c}$$
$$\left.\left.+\sqrt{(L_i-m_i-2)(L_i-m_i-n_j+m_j-2)}\begin{pmatrix} L_i-1 & L_i-n_j-2 & n_j+1 \\ m_i+2 & -m_i+m_j-1 & -m_j-1 \end{pmatrix}\right]\right\}$$
$$\times\frac{\sqrt{(2L_i-2)!}\begin{pmatrix} L_i & 1 & n_i \\ m_i-1 & 1 & -m_i \end{pmatrix}\begin{pmatrix} n_j+1 & 1 & n_j \\ m_j-1 & 1 & -m_j \end{pmatrix}}{\sqrt{(2L_i-1)(2L_i+1)(2L_i-2n_j-3)(2L_i-2n_j-1)(2L_i-2n_j-3)!}}$$

The coefficient $\widetilde{F}^{n_j,m_j}_{L_i;n_i,m_i}$ is given by

$$\widetilde{F}^{n_j,m_j}_{L_i;n_i,m_i}=(-1)^{n_j+m_i+1}\sqrt{\frac{\pi\,(2n_i+1)(2n_j-1)(2n_j+3)}{(2n_j-2)!}} \tag{E11}$$
$$\times[\,\widetilde{F}_1(n_j,m_j;L_i,n_i,m_i)+\widetilde{F}_2(n_j,m_j;L_i,n_i,m_i)+\widetilde{F}_3(n_j,m_j;L_i,n_i,m_i)\,]$$

where

$$\widetilde{F}_1(n_j,m_j;L_i,n_i,m_i)=\left\{\begin{pmatrix} L_i+1 & L_i-n_j & n_j+1 \\ m_i-2 & -m_i+m_j+1 & -m_j+1 \end{pmatrix}\right.$$
$$\times\sqrt{(L_i-m_i+2)(L_i-m_i+3)(L_i-m_i-n_j+m_j)(L_i-m_i-n_j+m_j+1)}$$
$$+\sqrt{(L_i+m_i)(L_i+m_i-n_j-m_j)}$$
$$\times\left[-2\sqrt{(L_i-m_i+2)(L_i-m_i-n_j+m_j)}\begin{pmatrix} L_i+1 & L_i-n_j & n_j+1 \\ m_i-1 & -m_i+m_j & -m_j+1 \end{pmatrix}\right. \tag{E11a}$$
$$\left.\left.+\sqrt{(L_i+m_i+1)(L_i+m_i-n_j-m_j+1)}\begin{pmatrix} L_i+1 & L_i-n_j & n_j+1 \\ m_i & -m_i+m_j-1 & -m_j+1 \end{pmatrix}\right]\right\}$$
$$\times\frac{\sqrt{(2L_i+2)!}\begin{pmatrix} L_i & 1 & n_i \\ m_i-1 & 1 & -m_i \end{pmatrix}\begin{pmatrix} n_j+1 & 1 & n_j \\ m_j-1 & 1 & -m_j \end{pmatrix}}{\sqrt{(2L_i+1)(2L_i+3)(2L_i-2n_j-1)(2L_i-2n_j+1)(2L_i-2n_j+1)!}}$$

$$\widetilde{F}_2(n_j,m_j;L_i,n_i,m_i)=-\left\{\begin{pmatrix} L_i+1 & L_i-n_j & n_j+1 \\ m_i-1 & -m_i+m_j+1 & -m_j \end{pmatrix}\right.$$
$$\times\sqrt{(L_i-m_i+1)(L_i-m_i+2)(L_i-m_i-n_j+m_j)(L_i-m_i-n_j+m_j+1)}$$
$$+\sqrt{(L_i+m_i+1)(L_i+m_i-n_j-m_j)}$$
$$\times\left[-2\sqrt{(L_i-m_i+1)(L_i-m_i-n_j+m_j)}\begin{pmatrix} L_i+1 & L_i-n_j & n_j+1 \\ m_i & -m_i+m_j & -m_j \end{pmatrix}\right. \tag{E11b}$$
$$\left.\left.+\sqrt{(L_i+m_i+2)(L_i+m_i-n_j-m_j+1)}\begin{pmatrix} L_i+1 & L_i-n_j & n_j+1 \\ m_i+1 & -m_i+m_j-1 & -m_j \end{pmatrix}\right]\right\}$$
$$\times\frac{\sqrt{(2L_i+2)!}\begin{pmatrix} L_i & 1 & n_i \\ m_i-1 & 1 & -m_i \end{pmatrix}\begin{pmatrix} n_j+1 & 1 & n_j \\ m_j-1 & 1 & -m_j \end{pmatrix}}{\sqrt{(2L_i+1)(2L_i+3)(2L_i-2n_j-1)(2L_i-2n_j+1)(2L_i-2n_j+1)!}}$$

$$\widetilde{F}_3(n_j,m_j;L_i,n_i,m_i)=\left\{\begin{pmatrix} L_i+1 & L_i-n_j & n_j+1 \\ m_i & -m_i+m_j+1 & -m_j-1 \end{pmatrix}\right.$$
$$\times\sqrt{(L_i-m_i)(L_i-m_i+1)(L_i-m_i-n_j+m_j)(L_i-m_i-n_j+m_j+1)}$$
$$+\sqrt{(L_i+m_i+2)(L_i+m_i-n_j-m_j)}$$
$$\times\left[-2\sqrt{(L_i-m_i)(L_i-m_i-n_j+m_j)}\begin{pmatrix} L_i+1 & L_i-n_j & n_j+1 \\ m_i+1 & -m_i+m_j & -m_j-1 \end{pmatrix}\right. \tag{E11c}$$
$$\left.\left.+\sqrt{(L_i+m_i+3)(L_i+m_i-n_j-m_j+1)}\begin{pmatrix} L_i+1 & L_i-n_j & n_j+1 \\ m_i+2 & -m_i+m_j-1 & -m_j-1 \end{pmatrix}\right]\right\}$$
$$\times\frac{\sqrt{(2L_i+2)!}\begin{pmatrix} L_i & 1 & n_i \\ m_i-1 & 1 & -m_i \end{pmatrix}\begin{pmatrix} n_j+1 & 1 & n_j \\ m_j-1 & 1 & -m_j \end{pmatrix}}{\sqrt{(2L_i+1)(2L_i+3)(2L_i-2n_j-1)(2L_i-2n_j+1)(2L_i-2n_j+1)!}}$$

Finally, the coefficient $\widetilde{g}^{n_j,m_j}_{L_i;n_i,m_i}$ is defined by

$$\widetilde{g}^{n_j,m_j}_{L_i;n_i,m_i}=(-1)^{n_j+m_i}\sqrt{\pi\,(2n_i+1)(2n_j-1)(2n_j+3)}\sqrt{\frac{(2L_i+2)!}{(2L_i-2n_j+1)!(2n_j-2)!}} \tag{E12}$$
$$\times[\,\widetilde{g}_1(n_j,m_j;L_i,n_i,m_i)+\widetilde{g}_2(n_j,m_j;L_i,n_i,m_i)+\widetilde{g}_3(n_j,m_j;L_i,n_i,m_i)\,]$$

where

$$\widetilde{g}_1(n_j,m_j;L_i,n_i,m_i)=\left\{\begin{pmatrix} L_i+1 & L_i-n_j & n_j+1 \\ m_i-2 & -m_i+m_j+1 & -m_j+1 \end{pmatrix}\right.$$
$$\times\sqrt{(L_i-m_i+2)(L_i-m_i+3)(L_i+m_i-n_j-m_j)(L_i+m_i-n_j-m_j+1)}$$
$$+\sqrt{(L_i+m_i)(L_i-m_i-n_j+m_j+1)}$$
$$\times\left[2\sqrt{(L_i-m_i+2)(L_i+m_i-n_j-m_j+1)}\begin{pmatrix} L_i+1 & L_i-n_j & n_j+1 \\ m_i-1 & -m_i+m_j & -m_j+1 \end{pmatrix}\right. \qquad \text{(E12a)}$$
$$\left.\left.+\sqrt{(L_i+m_i+1)(L_i-m_i-n_j+m_j)}\begin{pmatrix} L_i+1 & L_i-n_j & n_j+1 \\ m_i & -m_i+m_j-1 & -m_j+1 \end{pmatrix}\right]\right\}$$
$$\times\frac{\begin{pmatrix} L_i & 1 & n_i \\ m_i-1 & 1 & -m_i \end{pmatrix}\begin{pmatrix} n_j+1 & 1 & n_j \\ m_j-1 & 1 & -m_j \end{pmatrix}}{\sqrt{(2L_i+1)(2L_i+3)(2L_i-2n_j+1)(2L_i-2n_j+3)}}$$

$$\widetilde{g}_2(n_j,m_j;L_i,n_i,m_i)=-\left\{\begin{pmatrix} L_i+1 & L_i-n_j & n_j+1 \\ m_i-1 & -m_i+m_j+1 & -m_j \end{pmatrix}\right.$$
$$\times\sqrt{(L_i-m_i+1)(L_i-m_i+2)(L_i+m_i-n_j-m_j)(L_i+m_i-n_j-m_j+1)}$$
$$+\sqrt{(L_i+m_i+1)(L_i-m_i-n_j+m_j+1)}$$
$$\times\left[2\sqrt{(L_i-m_i+1)(L_i+m_i-n_j-m_j+1)}\begin{pmatrix} L_i+1 & L_i-n_j & n_j+1 \\ m_i & -m_i+m_j & -m_j \end{pmatrix}\right. \qquad \text{(E12b)}$$
$$\left.\left.+\sqrt{(L_i+m_i+2)(L_i-m_i-n_j+m_j)}\begin{pmatrix} L_i+1 & L_i-n_j & n_j+1 \\ m_i+1 & -m_i+m_j-1 & -m_j \end{pmatrix}\right]\right\}$$
$$\times\frac{\begin{pmatrix} L_i & 1 & n_i \\ m_i & 0 & -m_i \end{pmatrix}\begin{pmatrix} n_j+1 & 1 & n_j \\ m_j & 0 & -m_j \end{pmatrix}}{\sqrt{(2L_i+1)(2L_i+3)(2L_i-2n_j+1)(2L_i-2n_j+3)}}$$

$$\tilde{g}_3(n_j,m_j;L_i,n_i,m_i)=\left\{\begin{pmatrix} L_i+1 & L_i-n_j & n_j+1 \\ m_i & -m_i+m_j+1 & -m_j-1 \end{pmatrix}\right.$$
$$\times\sqrt{(L_i-m_i)(L_i-m_i+1)(L_i+m_i-n_j-m_j)(L_i+m_i-n_j-m_j+1)}$$
$$+\sqrt{(L_i+m_i+2)(L_i-m_i-n_j+m_j+1)}$$
$$\times\left[2\sqrt{(L_i-m_i)(L_i+m_i-n_j-m_j+1)}\begin{pmatrix} L_i+1 & L_i-n_j & n_j+1 \\ m_i+1 & -m_i+m_j & -m_j-1 \end{pmatrix}\right. \qquad \text{(E12c)}$$
$$\left.\left.+\sqrt{(L_i+m_i+3)(L_i-m_i-n_j+m_j)}\begin{pmatrix} L_i+1 & L_i-n_j & n_j+1 \\ m_i+2 & -m_i+m_j-1 & -m_j-1 \end{pmatrix}\right]\right\}$$
$$\times\frac{\begin{pmatrix} L_i & 1 & n_i \\ m_i+1 & -1 & -m_i \end{pmatrix}\begin{pmatrix} n_j+1 & 1 & n_j \\ m_j+1 & -1 & -m_j \end{pmatrix}}{\sqrt{(2L_i+1)(2L_i+3)(2L_i-2n_j+1)(2L_i-2n_j+3)}}$$

Acknowledgements

This work was performed under contract No. F04611-98-C-0005 with AFRL/PRRM Edwards AFB, CA, USA. We extend a special thanks to Dr. Gregory Ruderman for his support and helpful suggestions.

References

Vratsanos, L. A., Farris, R. J., 1993, A predictive model for the mechanical behavior of particulate composites. Part I: Model derivation; Part II: Comparison of model predictions to literature data, Polym. Eng. Sci, 33(22), 1458-1474.

Aravas, N., Xy, F., Sofronis, P., Namazifard, A., Fiedler, R., 2005, Constitutive response and damage in solid propellants, 41st AIAA/ASME/SAE/ASEE Joint Propulsion Conference, 10-13 July 2005, Tucson, Arizona, AIAA 2005-4348.

Chen, Y., Jiang, X., 1993, Nonlinear elastic properties of particulate composites, J. Mech. Phys. Solids 41, 1177-1190.

Christensen, R. M., 1979, **Mechanics of Composite Materials**, Wiley, New York.

Christensen, R. M., 1990, A critical evaluation for a class of micromechanics models, J. Mech. Phys Solids 38, 379-404.

Cusak, N. E., 1987, **The Physics of Structurally Disordered Matter,** Bristol: Hilger.

Buchalter, B. J., 1994, Orientational order in amorphous packings of ellipsoids, Europhys. Lett 26, 159-164.

Davis, I. L., Carter, R. G., 1990, Random particle packing by reduced dimension algorithms, J. Appl. Phys. 67 (2), 1022-1029.

Davis, I. L., Hatch, R. L., Yener, M., Chompooming, K., 1993. Stress and Strain Field in a Random Pack of Rigid Bonded Spheres, Phys. Rev. B 47(5), 2530-2545.

Davis, I. L., 1999, Particle pack influence on highly filled material properties, Current Opinion in Solid State & Materials Science 4, 505-513.

Edwards, R. H., 1951, Stress concentrations around spheroidal inclusions and cavities, J. Appl. Mech. 20, 19-30.

Eshelby, J. D., 1957, The determination of the elastic field of an ellipsoidal inclusion and related problems, Proc. Royal Soc A 241, 376-396.

Gent, A. N., 1980, Detachment of an elastic matrix from a rigid spherical inclusion, J. Mat. Sci. 15, 2884-2888.

Gent, A., Park, B., 1984, Failure processes in elastomers at or near a rigid spherical inclusion, J. Mat. Sci 19, 1947-1956.

Goodier, J. N., 1933, Concentration of stress around spherical and cylindrical inclusions and flaws, Appl. Mech**.,** APM-55-7, 39-44.

Hashin, Z., 1964, Theory of mechanical behavior of heterogeneous media, Appl. Mech. Rev 17, No. 1, 1-9.

Hashin, Z., 1983, Analysis of composite materials – a survey, J. Appl. Mech 50, 481-505.

Kochevets, S., Buckmaster, J., Jackson, T. L., Hegab, A., 2001, Random packs and their use in modeling heterogeneous solid propellant combustion, J. Propuls. Power 17 (4), 883-391.

Kushch, V. I., 1997. Microstresses and Effective Elastic Moduli of a Solid Reinforced by Periodically Distributed Spheroidal Particles, Int. J. Solids Structures, Vol. 34, No. 11, 1353-1366.

Lopez-Pamies, O., Ponte Castaneda, P., 2006, On the overall behavior, microstructure evolution, and macroscopic stability in reinforced rubbers at large deformations: I – Theory, II – Application to cylindrical fibers, J. Mech. Phys. Solids 54, 807-863.

Nunan, K. C., Keller, J. B., 1984, Effective elasticity tensor of a periodic composite, J. Mech. Phys. Solids 32, No. 4, 259-280.

Olsen, E. M., Rosenberg, J. D., Kawamoto, J. D., Lin, C. F., Seaman, L., XDT Investigations by Computational Simulations of Mechanical Response Using a New Viscous Intenal Damage Model, 11th International Detonation Symposium, Snowmass , CO, August 30-September 4, 1998 Office Of Naval Research ONR-33300-5, 170-178.

Phan-Thien, N., Kim, S., 1994, **Microstructure in elastic media: Principles and computational methods**, New York: Oxford University Press.

Robinson, K., 1951, Elastic energy of an ellipsoidal inclusion in an infinite solid, J. Appl. Phys 22, 1045-1054.

Sangani, A. S., Lu, W., 1987, Elastic coefficients of composites containing spherical inclusions in a periodic array, J. Mech. Phys. Solids, 35, No. 1, 1-21.

Sangani, A. S. and Mo, G., 1997, Elastic interactions in particulate composites with perfect as well as imperfect interfaces, J. Mech. Phys. Solids, 45, No. 11/12, 2001-2031.

Schapery, R. A., 1986, A micromechanical model for non-linear viscoelastic behavior of particle-reinforced rubber with distributed damage, Eng. Frac. Mech. 25, 845-867.

Shelley, J. F., Yu, Y., 1966, The effect of two rigid spherical inclusions on the stresses in an infinite elastic solid, J. Appl. Mech., 68-74.

Smith, J. C., 1974, Correction and extension of van der Poel's method for calculating the shear modulus of a particulate composite, J. Res. Nat. Bureau of Standards – A. Phys. and Chem. 78A, No. 3, 355-361.

Smith, J. C., 1975, Simplification of van der Poel's formula for the shear modulus of a particulate composite, J. Res. Nat. Bureau of Standards – A. Phys. and Chem. 79A, No. 2, 419-423.

Smith, J. C., 1976, The elastic constants of a particulate-filled glassy polymer: Comparison of experimental values with theoretical predictions, Polym. Eng. Sci. 16, No. 6, 394-399.

Smith, T. L., 1959, Volume changes and dewetting in glass bead-polyvinyl chloride elastomeric composites under large deformation, Trans. Soc. Rheo. III, 113-136.

Torquato, S., 1997, Exact expression for the effective elastic tensor of disordered composites, Phys. Rev. Lett. 79(4), 681-684.

Torquato, S., 2002, **Random Heterogeneous Materials, Microstructure and Macroscopic Properties**, Springer.

van der Poel, C., 1958, On the rheology of concentrated dispersions, Rheologica Acta, Band 1, Nr. 2-3, 198-205.

Varshalovich, D. A., Moskalev, A. N., Khersonskii, V. K., 1988, **Quantum Theory of Angular Momentum**, World Scientific.

Walpole, L. J., 1972, The elastic behaviour of a suspension of spherical particles, Quart. Journ. Mech and Applied Math. XXV, Pt. 2, 153-160.

Webb, M. D., Davis, I. L., 2006, Random particle packing with large particle size variations using reduced-dimension algorithms, Powder Technology 167(1), 10-19.